Ministry of Higher Education

and Scientific Research

University of Babylon

College of Science for Women

Department of Chemistry

Preparation Ag/TiO_2 Nano Material for the photo catalytic degradation of MG; optimization by Response Surface Methodology

A Thesis

Submitted to the Council of the College of Science for Women,
University of Babylon as a Partial Fulfillment of the
Requirements for the Degree of Master/
in Chemistry

by

Zainab Saleh Mahdi Najee

B.Sc., Chemistry of Science, University of Babylon (2001-2002)

Supervised by

Prof. Dr. Ayad Fadhil Alkaim

2023 A.D **1444 A.H**

بسم الله الرحمن الرحيم

﴿ عَلَّمَ الْإِنسَانَ مَا لَمْ يَعْلَمْ ﴾

صدق الله العلي العظيم

سورة العلق/ الاية 5

Dedication

To my family ,who buttress me ,my life and study….

ACKNOWLEDGEMENTS

My first thanks go to ***Allah*** (glory be to Him) who enabled me to complete this work and realize my first dream

I extend my sincere thanks to my supervisor ***Prof. Dr. Ayad Alkaim,*** for the proposal, guidance and assistance he provided in carrying out this work, It was an honor to be one of his students.

My thanks and appreciation go to ***Dr. Aseel Aljbeoree*** for her guidance , suggestion and support through the research work . Thanks to classmates (***Inaam Gouda, Ahemd Salah, Ishraq Taleb and Methal Ali)*** for their help and their beautiful and unforgettable situations.

Thank you to all the staff of Department of Chemistry at the College of Science for Women, University of Babylon.

Abstract

This thesis consists of three parts, The first part deals with synthesis of TiO_2 nanoparticles were synthesized by using the hydrothermal method, and doped with silver noble metal by a photo deposition on TiO_2 surface. Using commercially available aqueous solutions of titanium (IV) bis (ammonium lactate) di hydroxide in the presence of aqueous ammonia solution (3.00 M), anatase nanoparticles are made using a simple one-step hydrothermal method.. The chemical and physical properties of the prepared nanocomposites were characterized using different techniques such as X-ray diffraction (XRD) , Transmission Electron Microscopes (TEM), Field Emission-Scanning Electron microscopes (FE- SEM), Fourier transform infrared (FT-IR) spectroscopy, Energy Dispersive X-ray Spectroscopy(EDX), Thermal gravimetric analysis(TGA) ,UV-Visible spectroscopy.

Results show doping silver ions on the surface of TiO_2, did not show any new peaks for Ag in XRD characterization. The UV-visible technique showed that the energy gap of titanium dioxide was 3.23eV and it became less after doping silver 3.03 eV.

The second part deals with photo catalytic degradation of an aqueous solution of malachite green dye which has studied under different conditions in the presence of Ag /TiO_2 nanoparticles. The effect of various parameters such as effect of concentration of Malachite Green dye, effect of weight of Ag/TiO_2 Nano composite , light intensity , role of reactive oxygen species(ROS) ,effect regeneration experimental and Removal of laboratory sample (mixture of several dyes) from aqueous solution

The results explained the photo catalytic degradation efficiency which was increase by increasing the catalyst dosage from 0.1 g to 0.4 g also showed that the rate of photo catalytic degradation was elevated with the decreasing malachite green dye concentration. Photo catalysts made of Ag/TiO_2 have the ability to self-clean and be reused, which makes them effective and therefore promising for environmental remediation. The increase in light intensity also caused an increase in the rate of photo catalytic degradation and the role of H_2O_2 (hydrogen peroxide) as a scavenger and degradation for malachite dye.

The last part of this thesis is concerned with the Response Surface Methodology (RSM), which has been studied by using different concentrations of MG dye at different light intensities and amount of catalyst. The results show that the photo degradation efficiency has inversely been directed with the initial Dye concentration. It is also confirmed the observed the increase of light intensity leads to the increase of the photo degradation as a comparative between theoretical expected results and experimental results.

.

.

List of Content

List of Figures

List of Table

List of Symbols and Abbreviations

Symbols	Physical Meanings
C_t	Concentration After Different Time of Irradiation
CB	Conduction Band
e^-/h^+ pair	Electron-Hole Pair
eV	Electron Volt
NMs	Nanomaterials
E_g	Energy Gap
AOPs	Advanced Oxidation Processes
FE-SEM	Field Emission Scanning Electron Microscopy

Symbols	Physical Meanings
C_0	Initial Concentration
mW	Mille Watt
ROS	Reactive Oxygen Species
NPs	Nanoparticles
L. I.	Light Intensity
PDE	Photocatalytic Degradation Efficiency
FT- IR	Fourier Transform Infrared Spectroscopy
hν	The Photon Energy
TEM	Transmission Electron Microscopes
UV –Vis	Ultraviolet and Visible light
UV(A)	Ultraviolet light in the range from 315nm to 380nm
nm	Nano meter
VB	Valence Band
Temp	Temperature
λ	Wavelength
XRD	X- ray Diffraction
TiO_2	Titanium Dioxide
MG	Malachite Green
TGA	Thermal Gravimetric Analysis
EDX	Energy Dispersive x-ray Spectroscopy
Kapp	Apparent Photodegradation Rate Constant
JCPDS	Joint Committion Power Diffraction Standerd

Chapter One
Introduction

1.1 General Introduction

With rapid development of the economy and booming population growth, an enormous amount of resource (e.g. energy, food and water) is required in our society to sustain our activities. As a result, various kinds of pollution have. Among the various polluted problem produced [1]. Polluted water from industrial and agricultural activities can contain many metals and organic compounds such as dyes , the wide spread presence of organic dyes in industrial waste water come from the paper, textile and apparel industries result in substantial environmental contamination ,these dyes-polluted effluents comprise non-bio degradable ,highly poisonous and colored pigments that are harmful to living organism .Dyes are clearly visible in water even at very minute concentration (< 1ppm) and pollute aquatic environments which leads to incline to preclude light penetration and therefore, affect photosynthesis considerably[2-4]. Numerous dyes are difficult to remove from contaminated water solutions due to complex structure and synthesis. These dyes are not effectively removed by using traditional physical techniques such as ion exchange, coagulation, ozone treatment and membrane filtration , they are non-destructive and merely transfer contaminants from one phase to another. Moreover ,the biological treatments are often ineffective in removing or degrading the dyes [5-10] . New method for water treatment and improvements in the existing processes are needed to protect our environment Hetero generous photo catalysis. Nanotechnology has received wide attention from researchers through the past few decenniums. This interest is show in the large increase in the huge amount of Nano materials produced in the world[11, 12].

1.2 Nanomaterials

The basic and the key elements of nanotechnology are the nanomaterial, one of the main records of using nanoparticles in literature is dated back to the middle of the 19th century when Michael Faraday was studying gold colloids in the nanometer range. The nanomaterial with less than 100nm ones at least in one dimension, that means they have less size than that of micro scale physic chemical properties than the bulk material which in herently depends on their size and shape[13]Nanomaterial may be of different shape like nanorode, nanoparticle, nanosheet which can be characterized based on their dimensional. Nano particles show potential of many applications such as water treatment, agriculture, medical application, building material and there are several methods to produce NPs including condensation, corrosion , culture ionic and hydrothermal synthesis[14]

1.3 Classification of Nano materials

They are divided into different categories based on their size, which can range from 1 to 100 nanometers in at least one dimension, morphology, state, and chemical composition. Considering their general size and shape with respect to this material see Figure(1-1), Nano materials can be divided into four classes[15, 16].

1. Zero-Dimensional Nano materials(0-D) :

Nano materials possess all dimensions at the Nano scale range. i,e the size is less than 100nm which include spherical NMs ,cube , hollow sphere and core-shell NMs .

2. One-Dimensional Nano materials(1-D)

Nano materials are materials with one dimension not at the Nano scale while the other two dimensions at the Nano scale ,include metallic , nano filament, nanotubes , nanowires and Nano fibers.

3. Two-Dimensional Nano materials (2-D)

Nano materials only one of the dimension is located on the Nano scale while the other two are not, which include single-layered and multi-layered ,Nano films , Nano plates and Nano coating.

4. Three-dimensional Nano materials or bulk Nano materials (3-D):

Nano materials have various dimensions beyond 100nm ,3D NMs combine multiple Nano crystals in different direction. Example of the same foam, fibers, carbon Nano buds, poly crystal and layer skeleton.

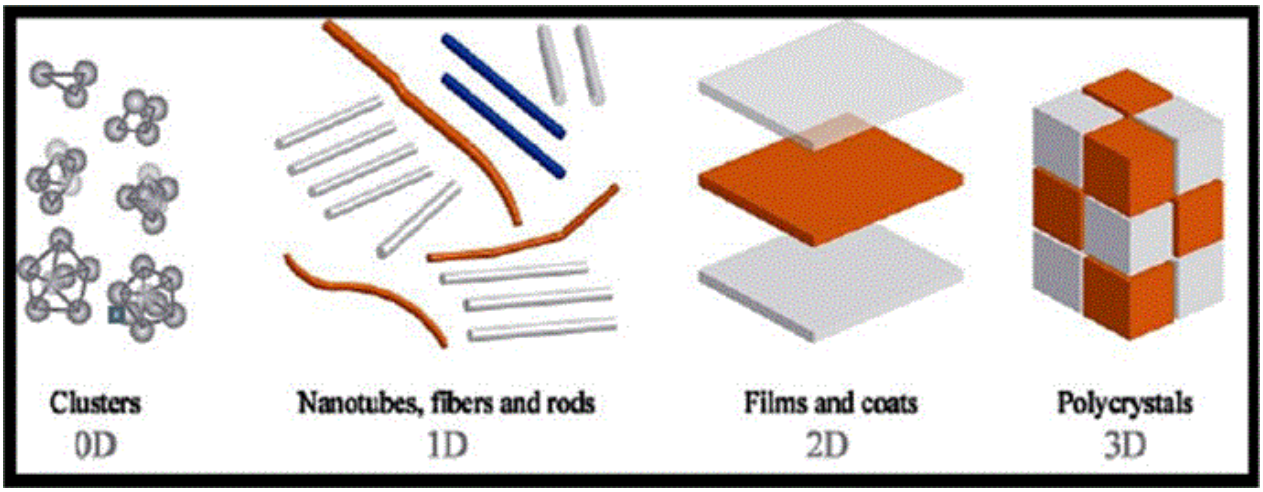

Figure(1-1) classification of Nano materials (0D ,1D ,2D ,3D)[17]

1.4 Synthesis Methods of Nano materials

There are a variety of techniques used to prepare metallic nanoparticles, and there are two main types: bottom-up techniques and top-down techniques.

1.Top down Method

In this method bulk material is converted into small nano-sized particles. Preparation of nanoparticles is based on size reduction of starting material by different physical and chemical treatment. It includes methods such as mechanical milling, ion sputtering, and laser ablation.

2. Bottom up Method

This method is based on formation of Nanoparticle from smaller molecules like joining of atoms, molecules or small particles. In this method, nanostructured building block of the nanoparticles first formed and then assembled to produce final nanoparticles. This includes the formation of NPs by the hydrothermal method, which is then followed by integration. Other examples include chemical reduction green synthesis, biochemical synthesis, physical and chemical vapor deposition [18]

1.5 Advanced Oxidation Processes (AOPs)

The removal of organic pollutants from wastewater are not effectively removed by using traditional techniques . Due to the synthetic pollutants' origin and the presence of complex aromatic structures, In order to go effectively remove the organic substrates, it is necessary to use safe products or methods that are less harmful to protect our environment . Heterogeneous photo catalysis, known as Advanced Oxidation Processes .One of the method for the degradation of harmful organic contaminants from air,soil and water [19]. These oxidation processes are

cost effective technologies and give rise to non-selective active species that oxidize a variety of non-biodegradable compounds. These processes have shown great potential in the treatment of pollutants, either in high or low concentrations. Figure 1-2. Schematic representation and classification of different treatments based on advanced oxidation processes (AOPs).Almost all AOPs are based on the generation of the reactive species ,hydroxyl radicals oxidation potential E^o 2.8eV. AOPs can produce the complete mineralization of pollutant to CO_2, water and inorganic compound as show in equations(1-1) and

(1-2)

$$AOPs \rightarrow OH^{\bullet} \quad (1\text{-}1)$$

$$Pollutant + OH^{\bullet} \rightarrow CO_2 + H_2O + \text{inorganic product} \quad (1\text{-}2)$$

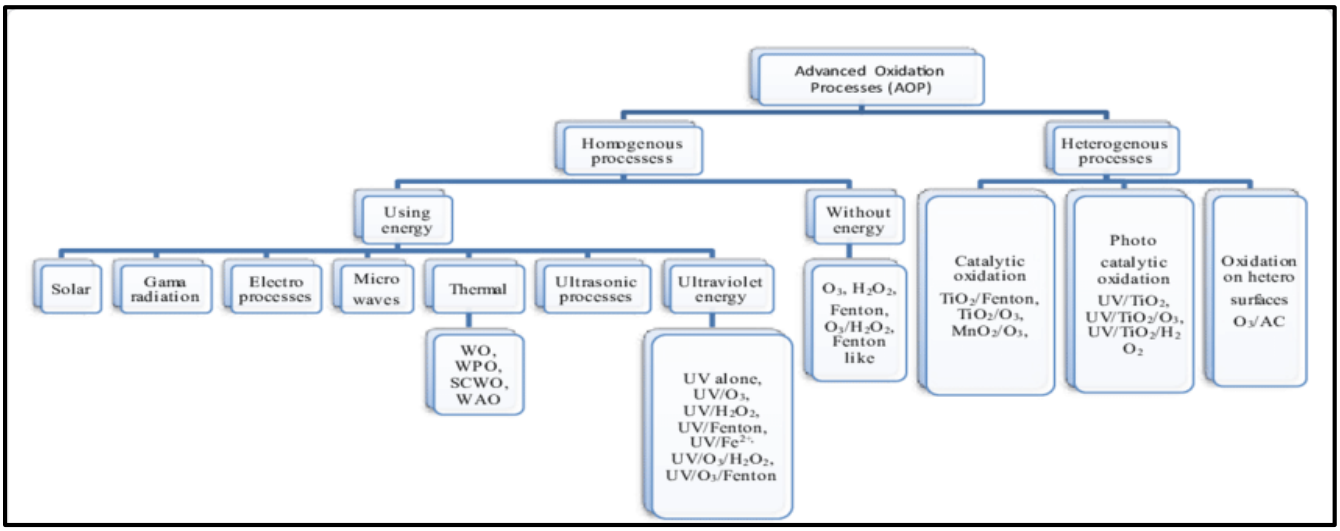

Figure (1-2): Schematic Representation and Classification of Different Treatments Based on Advanced Oxidation Processes (AOPs)[20]

1.6 Classification Advanced Oxidation Processes

1.6.1 Homogenous Photo Catalysis

This process occurs when both the semiconductor and reactant are the same phase i.e. gas, solid or liquid. It is possible to divided processes that use energy

and processes that do not use energy (chemical oxidation) . All processes generate OH radicals, which are highly reactive and attack the majority of organic molecules[21]

1.6.2 Heterogeneous Photo Catalysis

Heterogeneous photocatalytic is one of the advanced oxidation processes used for removal of organic dyes , in this type , the reactant and semiconductor will be found in different phase. The photo catalysis is a process in which semiconductor absorbs light energy to form radicals in the solution ,these radicals can be formed from the molecule itself and are capable of oxidizing or reducing destroying the target contaminants. The oxidizing species, either bound hydroxyl radicals or free holes, are generated[22] as shown in Figure (1-3)

Organic dyes can be completely mineralized reacting with oxidizers to form CO_2 and water without generated any harmful by-product[23]. Heterogeneous photocatalytic has attracted much attention as it is a new purification technique for air and liquid[24, 25]

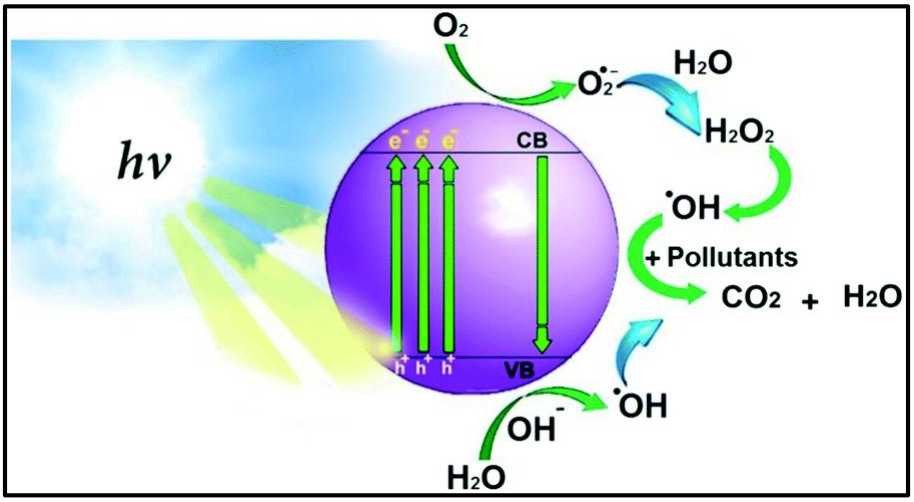

Figure (1-3) General Important Events That Take Place on an Irradiation Semiconductor Particle[19]

1.7 Dyes

Dyes are an organic chemical which on binding with materials, it will give a colour to the materials. The colour of a dye is provided by the presence of a chromophore group. A chromophore is a configuration consisting of conjugated double bonds containing delocalized electrons.

Other common chromophore configurations include azo (-N=N-), carbonyl (-C=O); carbon (-C=C-); carbon-nitrogen (>C=NH or -CH=N-); nitroso (-NO or N-OH); nitro(-NO_2 or =NO-OH); and sulphur (C=S). The chromogen, which is the aromatic structure normally containing benzene, naphthalene or anthracene rings, is part of a chromogen-chromophore structure along within an auxo-chrome [26, 27].

1.7.1 Malachite Green(MG)

Malachite green is an organic compound that is used as a dyestuff and controversially as an antimicrobial in aquaculture.So, the chemical structure of Malachite Green(MG) was shown in Figure (1-4). Malachite green is traditionally used as a dye for materials such as silk, leather, and paper. Despite its name the dye is not prepared from the mineral malachite; the name just comes from the similarity of color [28].

Its application extents in the aquaculture, commercial fish hatchery and animal husbandry as an antifungal therapeutic agent, while for human it is used as antiseptic and fungicidal. However, its oral consumption is carcinogenic. The available toxicological information reveals that in the tissues of fish and mice MG easily reduces to persist able leuco-Malachite Green, which acts as a tumour promoter. Thus, the detection of MG in fishes, animal milk and other food stuff designed for human consumption are of great alarm for the human health. Studies

also confirm that the products formed after the degradation of Malachite Green are also not safe and have carcinogenic potential. Thus it becomes necessary to remove such a toxic dye from wastewater before it released into aquatic environment. [29]

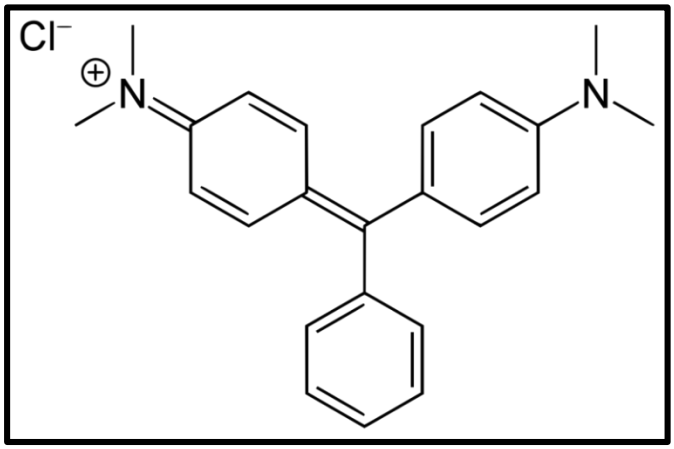

Figure (1- 4): Chemical Structure of Malachite Green(MG)[30]

1.8 Semiconductor

Semiconductor types, such as TiO_2, ZnO, CdS, and ZnS, can act as sensitizers for light-induced redox processes because of the electronic structure of the metal atoms in the chemical combination. This is demonstrated by the filled valence band (VB) and an empty of a conduction band(CB). For a substance to be regarded as a semiconductor, the valence band and conduction band must both be separated by an energy gap, or band gab. When a semiconducting molecule absorbs photons with energy equal to or greater than its band-gab, electrons in the valance band can be excited and then jump up into the conduction band and thus charged carrier are generated[31]. TiO_2 is the most widely used semiconductor in the photo catalysis processes.

1.9 Structure and Crystal Morphology of TiO_2

Titanium dioxide exist in three crystalline phases: rutile, anatase, and brookite . The anatase structure has a band gap energy of 3.2 eV and absorbs ultraviolet radiation. The rutile structure has a band gap of 3.0 eV and absorbs ultraviolet rays, as well as radiation that is slightly closer to the visible spectrum. The third structure, brookite, has a band gap of 2.96 eV and absorbs wavelengths close to the visible spectrum. The brookite structure is not used in industrial applications[32, 33] Both rutile and anatase structures can be described in terms of chains of TiO_6 octahedral, where each Ti^{4+} ion is surrounded by an octahedron of six O^{2-} ions. Figure (1-5) shows the unit cell structures of the rutile and anatase TiO_2. The difference is in the distortion of two crystal structures of each octahedron and by the assembly pattern of the octahedra chains. It is observed in rutile that the octahedron shows a slight orthorhombic distortion, while anatase showed that the octahedron is significantly distorted so that its symmetry is lower than orthorhombic.

The Ti-O distances in anatase are shorter, whereas the Ti-Ti distances are larger than those in rutile. In the structure of rutile, each octahedron is in contact with 10 neighboring octahedrons (two sharing edge oxygen pairs and eight sharing corner oxygen atoms), while, in the structure of anatase, each octahedron is in contact with eight neighbors (four sharing an edge and four sharing a corner). The difference in mass densities and electronic band structures lead to difference in lattice structures between the two forms of TiO_2[34].

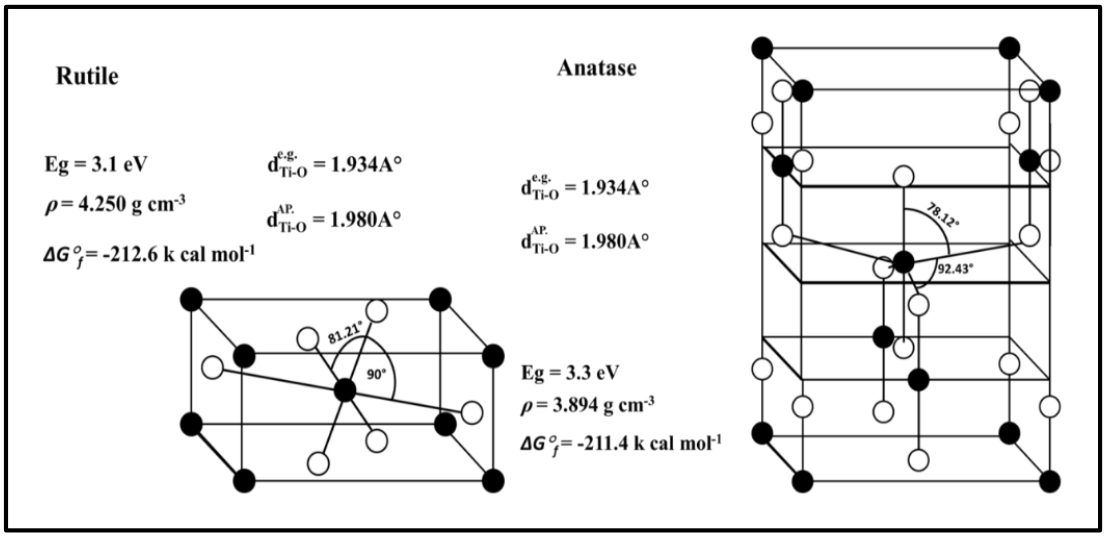

Figure (1-5): Lattice Structure of Anatase and Rutile TiO_2-NPs[34]

1.9.1 Chemical and Physical Properties of TiO_2

Titanium dioxide is a substance that is used in the production of paint and paper because of its white colour, chemical stability, and lack of danger. This implies that it contributes to the healthy production of tooth paste and its composition. The following list of TiO_2's chemical and physical characteristics[35].

1.Titanium (59. 95%) and oxygen (40.05%) make up the majority of the molecular weight of TiO_2 (79.86 g/mol). The boiling point is(2,972^{o}C) and the melting point is(1,843^{o}C)[36] .

2.TiO_2 is a semiconductor ;it is one of the Transparent Conducting Oxide Semiconductors (TCOs) and high optical transmittance in the visible region [37].

3.TiO_2 is insoluble to water ,therefore, it is used in an industry as a pigment in paint, sunscreen and some kinds of shampoo and food coloring.

4 . The anatase TiO_2, which is a low temperature phase, generally considered to have the highest photocatalytic activity because of its comparatively high density of surface oxygen. Additionally, due to the indirect band gap of anatase TiO2, it exhibits longer charge carrier life time compared to the rutile, which is a direct band gap material[38]

5.Titanium dioxide has a strong n-type conductivity that allows electrons to move as charge carriers in the conduction band ,this is mainly due to a large number of original defects, such as oxygen vacancies. oxygen interstitials, titanium interstitials, and titanium vacancies. These oxygen vacancies and titanium interstitials responsible for n-type conductivity[39, 40] .

1.9.2 Synthetic Methods for TiO_2 Nanostructures

There are a number of available technique for the synthesis of titania nanoparticles these synthesis methods are highlighted in the following subsection .The method used plays a significant role in the shape ,size and photochemical properties of TiO_2 .In order to prepare the nanostructures shown in Figures 1-6, the standard synthetic methods have been developed. A method for producing Nano sized TiO_2 with anatase phase has been the hydrothermal process[41]

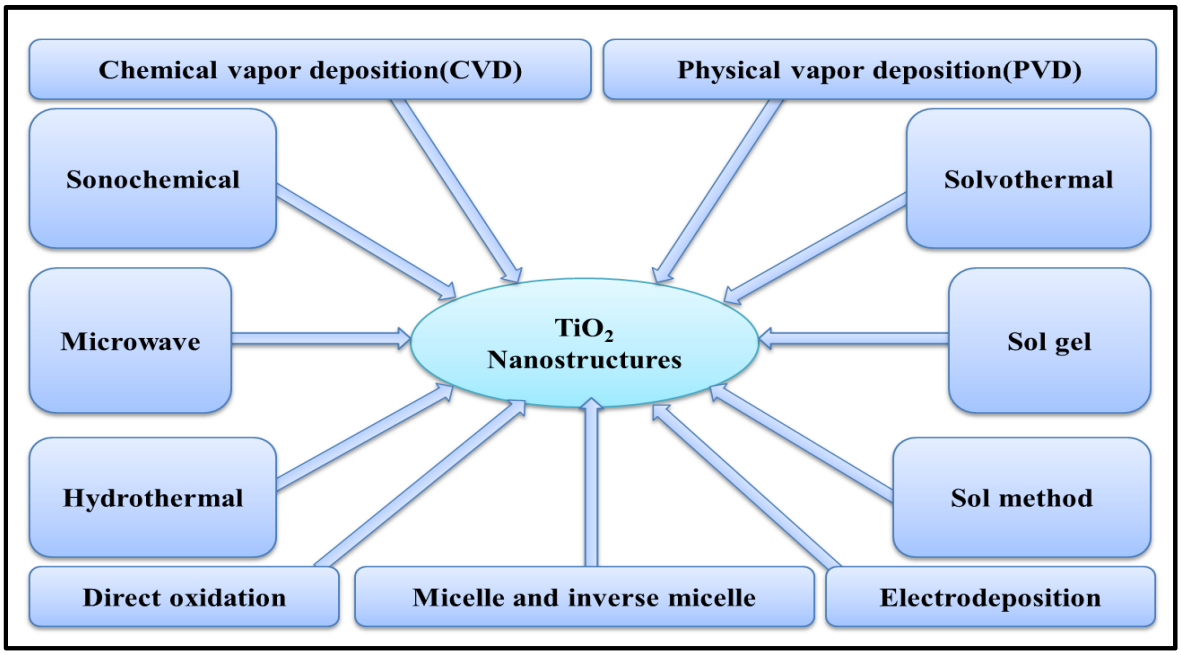

Figure (1-6): Common Synthetic Methods of TiO_2 Nanostructures

1.9.2.1 Hydrothermal Method

Hydrothermal synthesis is one of the most commonly used method for preparation of nanomaterial by using single or heterogeneous phase reactions in aqueous media at high temperatures (T>25 ^{o}C) and pressures (P>100 k Pa) [42]. In the middle of the 19th century, hydrothermal research was first conducted. It depends on the solubility of aqueous solution under hot water and higher temperature level in steel pressure vessels called autoclaves.

The process requires the constant maintenance of a temperature difference between the two ends of the crystallizing compartment, with the higher temperature end being where the solvent dissolves whenever it occurs and the lower temperature end being where the nanoparticle growth (TiO2 partial) occurs .[43]

One of the main advantages of hydrothermal method is economies. Another important advantage of the hydrothermal synthesis is that the purity of hydrothermally synthesized powders significantly exceeds the purity of the starting materials .Perhaps because hydrothermal crystallization is a self-purifying process during the growing crystals /crystallites tend to reject impurities present in the growth environment. The impurities are removed from the system together with the crystallizing solution[44, 45] .The resulting nano crystals are empty defect-free with high specific surface area, low agglomeration between particles, good crystallinity, crystal symmetry, narrow particle size distribution, formation of anatase, low energy consumption, and inexpensive instrumentation [46]

1.9.3 Photo Catalytic Degradation

A semiconductor photo catalyst is excited by near ultraviolet light (380 nm) during a photocatalytic reaction, which modifies the reaction without using the semiconductor photo catalyst as a reactor.Photo catalysis is significantly influenced by the type and size of the photo catalyst. energy in the band gap

activate the catalyst should be correlated with the wavelength of light source. As size decreases, the specific surface area of photo catalyst illuminated and contact area of photo catalyst with reaction medium increases [47]. The basic mechanism of the photocatalytic process is when photons of a light source with an energy greater than or equal to its band gap energy (E_g) of TiO_2 catalyst ,electrons get excited from the valence band VB to the conduction band CB leaving holes in the VB which generation of the electron - hole pair

$$TiO_2 + h\upsilon\ (UV) \rightarrow e^- CB + h^+ VB \qquad (1\text{-}1)$$

Dye molecules absorb photons and get energetically excited from their highest occupied molecular orbital (HOMO) to lowest unoccupied molecular

$$Dye + h\upsilon \rightarrow Dye^{*} \quad (1\text{-}2)$$

Then, photo generated electrons react with O_2 absorbed on the catalyst surface or dissolved in water, producing $O_2^{\bullet-}$

$$e^- + O_2 \rightarrow O_2^{\bullet-} \quad (1\text{-}3)$$

Formation of superoxide radical through transfer of electron from the excited state of dyes to the conduction band of catalyst or can be transferred to the oxygen

$$Dye^{*} + O2 \rightarrow O2^{\bullet-} + Dye^{+} \quad (1\text{-}4)$$

Photo generated holes can oxidize dye to form Dye^+ ,or react with OH^- or H_2 O oxidizing them into $OH^{\bullet}$.

$$Dye + h^+ \rightarrow Dye^+ \quad (1\text{-}5)$$

$$(OH^- \text{ or } H_2O) + h^+ \rightarrow OH^{\bullet} + H^+ \quad (1\text{-}6)$$

After formation reactive hydroxyl radicals $OH^{\bullet}$, superoxide anion$O_2^{\bullet-}$ which necessary for the oxidation and subsequent mineralization of the organic contaminants.

$$Dye + OH^{\bullet} \text{ or } O_2^{\bullet-} \rightarrow \text{simple product} \quad (1\text{-}7)$$

The redox reaction of the (e^-/h^+) pairs on the surface of TiO_2 catalyst play an essential role in enhancing the rate of degradation [48, 49].

1.9.4 Ag/TiO_2 Nanoparticles

The Titanium oxide low efficiency under solar radiation due to its wide band gap and fast electron-hole recombination. Noble metal nanoparticles, such as Pd , Pt , Au, and Ag as shown in Figure(1-7) have been to be very effective for

enhancement of TiO_2 photo catalytic. Among them, Ag is the most potential photo catalysts used in doping TiO_2 due to novel effect on the improvement of photo activity of semiconductor photo catalysis and lower cost . Ag loading TiO_2 is commonly used to reduce band gap energy and reduced recombination between electron-hole pairs at the photo catalyst . The incorporation of Ag^+ in TiO_2 establishes the Schottky barrier that behaves like an electron trapper, which renders electron recombination and thus stabilizes charge separation . Ag^+ reduces to Ag^0 upon exposure to sunlight, but it still acts as electron acceptor centers, thus prevents the charge recombination. Moreover, Ag^0 clusters enhance the visible light absorption on the TiO_2 surface due to the surface Plasmon resonance (SPR) effect. These two phenomena effect synergistically, resulting in high photocatalytic performance [50, 51]. A small amount of Ag is sufficient to enhance the reactivity; however, a large amount of silver metal acts as recombination centers that prevent the production of a large of radicals and reduce the lifetime of the photo catalyst[52]

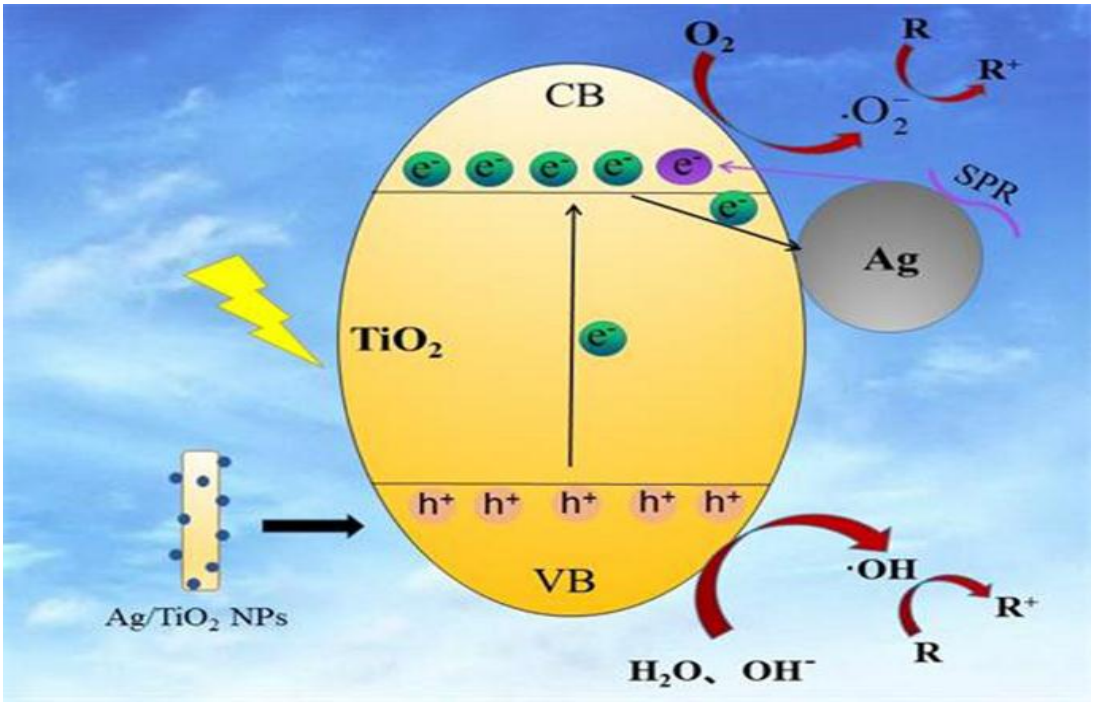

Figure (1-7) :Photo Deposition of silver on the TiO_2 surface [53]

1.10 Application for Removal of Dyes by Using Different Surfaces

- ***M Hirano et al.*** **(2002)** Synthesized titania TiO_2 nanoparticles doped with zirconia ZrO_2 by hydrolysis under mild hydrothermal condition at 200C° and 240C° followed by annealing at 400-1100C° .The sample characterized by XRD and TEM , lattice crystalline growth is observed in ZrO_2-doped TiO_2 with an anatase type structure under high temperature[54]
- ***P Falaras et al.*** **(2003)** prepared Ag-TiO_2 by immobilized on glass substrate . Based on SEM, AFM,SEM picture confirmed the existence of an open porous of interconnected titania particles on the semiconductor surface ,AFM analysis proved presence of spherical silver particle on the catalyst .The sliver deposition condition were optimizing maximum photo catalytic efficiency which increase in photo degradation of methyl orange ,a well know azo - dye pollutant in the textile industry[55].

- ***A Orlov et al*. (2004)** TiO_2 modified by gold was prepared by deposition of precipitation method .The result indicate that gold particle size is an important parameter ,at very low metal loading gold nanoparticles enhance the catalytic activity of p25 titania towards the photo degradation of 4- chloro phenol and the highest gold loading causes of the rate of photo degradation decrease [56]
- ***G Hayes et al*. (2005)** Co doped TiO_2 nanoparticle were synthesized by sol-gel and dip-coating techniques .Several analytical tools such as XRD,TEM,XPS,EDAX were used to investigate the nanoparticle structure, size distribution and composition .Result obtained that the rutile to anatase concentration ratio increases with increase of the cobalt dopant concentration annealing temperature ,the activation energy for the phase transformation anatase to rutile was measured 229,222,211KJ/mol for 0.008,0.1 ,0.2mol Co in TiO_2 [57]
- ***Jang et al*. (2006)** CdS nanoparticles which deposited on TiO_2 Nano sheets was synthesized by hydrothermal treatment ,CdS/TiO_2 high activity for decomposition of methylene blue under visible light $\lambda \geq 420$ nm[58]
- ***S Rengaraj et al*. (2007)** TiO_2 and Ag/TiO_2 catalyst were prepared by an Ultrasonic assisted sol-gel method .The as-prepared sample were characterized by XRD, TEM , EDX, XPS, visible absorption spectra and optical ellipsometry .Practically that the presence of Ag on TiO_2 catalyst could enhance the photo catalytic oxidation of chloro phenols in an aqueous suspension[59]
- ***W Wang et al*. (2008)** Fe^{3+} doped core-shell-type $Ag@TiO_2$ Nano particle have been prepared by hydrothermal method .The result showed that $Ag@TiO_2$-doped Fe^{3+}extend their absorption into visible region, experimental found Fe^{3+} ions could stability the $Ag@TiO_2$ colloid by holding back the aggregation of the core-shell nanoparticles[60]

- ***H Y Chuang et al*. (2009)** Discrete Ag@TiO_2 and NiAg@TiO_2 nanoparticles were prepared by the reduction of Ag^+/Ni^+ ions followed by sol-gel coating of TiO_2 to form Ag/TiO2 and Ni Ag/TiO_2 Nano particle which have posses significantly higher photo catalytic activities than TiO_2 nanoparticle in the visible light region towards rohodamine B, while TiO_2 has high activities than Ag/TiO_2 and Ni Ag/TiO_2 in the UV light. Based on TEM analysis revealed that their core diameter 6.5 and 7.5nm,and their shell thicknesses were 2.5 and 2.8nm respectively[61].
- ***Q Xiang et al*. (2010)** Plasmatic photo catalytic Ag/TiO_2 Nano composite prepared under microwave-hydrothermal condition ,followed by photochemical reduction process under xenon lamp irradiation . SEM images showed that of pure TiO_2 and Ag/TiO_2 Nano composite hollow sphere with the size of ≈ 500nm ,results show a highly surface effective and photo catalytic degradation for(Rh B)[62]
- ***AA Ashkarran et al.* (2011)** Ag/TiO_2 Nano composite with various silver contents was synthesized by sol-gel and the novel arc discharge method in liquid. The result Ag/TiO_2 Nano particle significantly enhanced antibacterial activities and photo catalytic activity were demonstrated for the inactivation E-coli bacteria and Rh B under visible light ,when 0.15gr Ag/TiO_2 nanoparticles revealed best antibacterial activity while 0.05gr Ag/TiO_2 nanoparticles highest photo catalytic efficiency [63]
- ***D wang et al*. (2012)** TiO_2 loaded with crystalline Nano silver (c- Ag/TiO_2) was synthesized by a one-step low-temperature hydrothermal method using tetra-n-butyl titanate and $AgNO_3$ as precursors .The result show that the Nano silver particles of Ag/TiO_2 prepared by hydrothermal are crystalline ,while they amorphous when prepared by the conventional UV reduction deposited method and the photocatalytic activity of c-Ag/TiO_2 found to have improvement for H2S

degradation being more than 2 times over the prepared by the conventional method [64]

- ***Alkaim et al.* (2013)** Studied the photocatalytic degradation of EDTA by using Pt/TiO_2, the surface of material investigate by using TEM; SRX and FE-SEM. Results show very high productivity of H_2 gas by using synthesized surface[65].
- ***Y Yang et al.* (2014)** TiO_2 -graphene (P_{25} – GR, PG) Nano composite was synthesis by hydrothermal method and then Ag nanoparticles (Ag NPs) was assembled in P_{25}GR (Ag -P_{25}- GR, APG) .The result show the degradation efficient of pure P_{25}can hardly activated in the visible region , the efficiency only about 7% , while degradation efficiency of PG is about 17% which should be presence of GR that improve light absorption intensity and enhanced trans portion of photo generated charge carrier , the efficiency of APG is about 45% which due to surface Plasmon resonance SPR , also The cross ponding hydrogen evolution rate of APG prepared with 0.002M $AgNO_3$ was 7.6 times than pure P_{25} and 2.7 times than PG in the test condition due to PG and SPR effect[66]
- ***Z Lian et al.* (2015)** Hierarchical TiO_2 Nano tube arrays (H-TiO_2-NTAs) with macro porous structure were prepared through two step method based on electrochemical iodization ,Ag quantum dots Ag QDs with tunable size(1.3-21.0nm) deposited by pulse electrode method . The as-obtained Ag/H-TiO_2 NTAs exhibited strong visible – light absorption capability , high photo current density and enhanced photo electro catalytic activity toward photo electro catalytic hydrogen evolution under visible - light irradiation (λ>420nm)[67]
- ***L Goa et al.* (2016)** Ag –TiO_2 hetero structure with Ag Nano particle and TiO_2 particle well-grown on wood substrate by a two-step combining hydrothermal synthesis and silver mirror reaction .The morphology of Ag/TiO_2 -coated wood by SEM, TEM, FT-IR, XRD, the result of TEM show that the Nano particles of

Ag are clearly visible ,making the wood surface rough , generation of dual-size surface structure on the wood .The Ag/TiO_2-coated wood posses .The modified wood has potent antibacterial activity toward both Gram-positive and Gram – negative bacterium .The multifunctional film coated on wood surface a good photo degradation of organic pollutant [68]

- ***K Saeed et al.*** **(2017)** titanium oxide supported palladium TiO_2 /Pd and titanium oxide supported platinum TiO_2/Pt nanoparticles were prepared through the incipient wetness method .Based on SEM and EDS, The SEM images shows that Pd and Pt nanoparticle appeared on the surface of the TiO_2 ,the size range of both TiO_2 /Pd and TiO_2 /Pt where below 500nm ,while photo degradation of methyl violet was performed by UV/VIS spectra photo metery .Both TiO_2 /Pd andTiO_2 /Pt nanoparticles were used as photo catalyst for the photo degradation of methyl violet in aqueous media under UV light irradiation .The various parameters such as catalyst dosage ,concentration of dye and medium effects on the photo catalytic degradation[69]
- ***H Mozafari et al.*** **(2018)** $CoFe_2O_4$nanostructue were synthesized by precipitation method ,the $CoFe_2O_4$-TiO_2 Nano composite were prepare using the sol –gel method , the silver nanoparticles were produced by reducing agent ($AgNO_3$) with $NaBH_4$,by adding reducing agent,$CoFe_2O_4$-TiO_2-Ag was produced by a simple precipitation method .The photocatalytic activity of the Nano composite was evaluated monitoring the degradation of organic dyes in an aqueous solution under UV irradiation .The dye concentration decreased rapidly with an increase in the UV irradiation time of organic dye decompose carbon dioxide , water and other less toxic or non toxic (residual)[70]
- ***D Hong et al.*** **(2019)** Ag@TiO_2 Nano particles with Ag metal cores and TiO_2 semiconductors shells were prepared with a hydrothermal method .The core – shell Ag@TiO2 were dispersed on glass plates and annealed at 500C_o to remove

carbon residues and used as photo catalyst for CO_2 conversion by irradiation of solar simulator (AM1.5) under CO_2 atmosphere, CH_4 evolution by CO_2 photo conversion .The role of Ag@TiO_2 core-shell was also demonstrated in photodecomposition Rhoda mine B . Utilization of UV-Vis spectrometer to determine the rate of dye degradation by each catalyst[71]

- ***N Guy et al.*** **(2020)** Ag/Ag_3 VO_4/TiO_2 Nano composites were prepared by a three step process including hydrothermal ,precipitation and photo reduction .The Ag/Ag_3 VO_4/TiO_2 nanocomposites demonstrated increased visible light absorption and photo catalytic efficiency in degradation of Rhodamine B The degradation was detected 97.3%in 45min under visible light ,compared with Ag_3VO_4 ,TiO_2 ,Ag_3 VO_4/TiO_2 ,Ag/Ag_3 VO_4/TiO_2 exhibited the highest efficiency owing to synergetic effect between Ag_3 VO_4,TiO_2 and surface plasmon resonance effect of Ag nanoparticle to elimination of organic pollutants[72]
- ***G Zhang et al.*** **(2021)** AgCl/Ag/TiO_2 hybrids were prepared by impregation-hydrolyzation –calcination method combining with photo-reduction .Based TEM,SEM result showed that the as- prepared AgCl/Ag/TiO_2 hybrid possessed hierarchical tube structure and the template of fluff of chinar tree was crucial in inducing and assembling the unique structure of AgCl/Ag/TiO_2 Nano sheet and exhibited favorable photo catalytic activity and good stability to degrading 96% tetra cycline hydrochloride under visible –light irradiation ,the result trapping experiment indicate that the $O_2^{-\bullet}$ radicals are the vital active species of oxidation during the photo catalytic degradation process[73]
- ***F S Razavi et al.*** **(2022)** TiO_2 prepared by sol-gel method ,BaF_{12} O_{19} synthesized by micro wave and sol-gel combustion (using green fuel ,glucose) method .Pt and Pd were deposit on BaF_{12} O19/TiO_2 by reducing agent (glucose, green surfactant) under ultra sound wave. On the basis of XRD and SEM results ,the

composite are highly and impurity-free .BaF_{12} O_{19}/TiO_2 @Pt and BaF_{12} O_{19} /TiO_2 /Pd Nano composite were used to degrade anionic and cationic dyes under

Visible irradiation,the TiO_2 and evaluates their feasibility for waste water treatment(paracetamol was chosen as the model pharmaceutical pollutant) and hydrogen gas generation, the highest percentage degradation to methyl orange 96% and 92% respectively [74].

- ***Y Cherif et al*. (2023)** Meso porous titania was prepared by the hydrothermal – assisted sol-gel method and silver Ag nanoparticles impregnated with meso porous experimental result showed that the decorated anatase TiO_2 nanoparticles (size80 and 100nm) with 5nm Ag nanoparticles induced visible –light absorption and enhanced charge carrier separation .As a result 0.01g/L Ag/TiO_2 effectively removed 99% of .01g/L paracetamol in 120min and exhibited 60% higher photo catalytic removal than pristine TiO_2 and hydrogen generation [75]

1.11 Aim of the Study

In order to investigate the role of synthesized TiO_2 nanoparticles as a photocatalytic systems and Ag/TiO_2 nanoparticles, this study has been set to achieve the following:

1. Preparation of pure TiO_2 Nanoparticles by hydrothermal method.
2. Preparation of binary Ag/TiO_2 Nanocomposites by photo deposition method.
3. Role of doping Ag on the surface of TiO_2 to enhance the activities of binary nanocomposites in the photocatalytic degradation of Malachite green dye .
4. Studying photo catalytic activity under different condition such as mass of catalyst, MG dye concentration, light intensity, roles of reactive oxygen species ROS, regeneration experiments and removal of laboratory sample (mixture of several dyes) from aqueous solution.
5. Study of response surface methodology (RSM).

Chapter Two

Experimental part

2.1 Chemicals

The chemicals used in this work are listed in Table (2-1). All chemicals were used without further purification.

Table (2-1): Chemicals for all component

NO.	Chemicals	Chemical formula	Supplier	Purity %
1	Titanium(IV) bis(ammonium lactate)dihydroxide	$C_6H_{22}N_2O_8Ti$	Sigma-Aldrich	99.0
2	Aqueous ammonia	NH_3	Sigma-Aldrich	36.0
3	Methanol	CH_3OH	Alpha Chemika	98.0
4	Ethanol	CH_3CH_2OH	Alpha Chemika	98.0
5	Silver nitrate	$AgNO_3$	Sigma-Aldrich	99.0
6	Malachite green	$C_{23}H_{25}CLN_2$	Sigma-Aldrich	99.0
7	Hydrogen Peroxide	H_2O_2	Sigma-Aldrich	35%

2.2 Instruments and Equipment

The instruments used in this study with their company are listed in Table (2-2).

Table (2-2): The list of Instruments was used in this project.

No.	Instrument	Company supplied	Location of current measurement
1	UV-Visible spectrophotometer, Single beam	Shimadzu, Japan	University of Babylon / College of science for women
2	UV-Visible spectrophotometer, Double beam	Shimadzu, Japan	University of Babylon / College of science for women
3	Band gap energy measurement	UV/ Visible Shimadzue 2700	University of Babylon / College of science for women
4	LED/ UVA specific wavelength 365 nm	USA/ Thorlab company	University of Babylon / College of science for women
5	Field-Emission Scanning electron microscope (FE-SEM)	TESCAN ,Czechia Republic	University of Tehran
6	Transmission electron microscope (TEM)	Leo, Germany	University of Tehran
7	X-Ray diffraction (XRD)	Japan	The Ministry of Science and Technology
8	Fourier – Transform (FTIR)	Shimadzu, Japan	University of Babylon / College of science for women
9	Thermal gravimetric analysis(TGA)	Shimadzu, Japan	University of Babylon /College of science for women

No.	Instrument	Company supplied	Location of current measurement
10	Hydrothermal System	Germany	University of Babylon /College of science for women
11	Centrifuge	JANETZI - T5, Belgium	University of Babylon / College of science for women
12	Ultrasonic cleaner (power sonic 420)	Hwashin, Korea	University of Babylon / College of science for women
13	Oven	Labtech, Korea	University of Babylon / College of science for women
14	Sensitive balance	Denver instrument , Germany	University of Babylon / College of science for women
15	Irradiation Solar light "wavelength 365-600 nm"	Commercial source	University of Babylon / College of science for women

2.3 Preparation Titanium Dioxide Nanoparticle

Titanium dioxide nanoparticles were prepared by thermal hydrolysis of titanium(IV) bis (ammonium lactate) di hydroxide (TALH), and these experiment was carried out in a 150 mL Teflon cup enclosed in a stainless steel autoclave (Berghof, DAB-3). In all experiments, 10 mL of titanium (IV) bis (ammonium lactate) di hydroxide aqueous solution, in the presence 15ml of an aqueous ammonia solution with 40 ml ethanol, were mixed, followed by the addition of distilled water to reach the final volume of 115 mL. Then this solution was mixed very well by put on magnetic stirring for further 30 minutes. The resulting solution

was transferred into the Teflon cup . Afterward the Teflon cup was sealed in the autoclave, which was closed and placed into an electric furnace held at 160 °C for 24 hr . Finally, the autoclave was cooled down to ambient temperature and the resulting powder was washed several times with distilled water until pH is equal to 8.1 with Ultrasonic device and dried overnight in an oven at 60°C as appear in Figure (2-1) .The powder obtained is subjected to annealing at temperatures 500 °C for 2h in furnace to yield TiO_2 Nano particles.

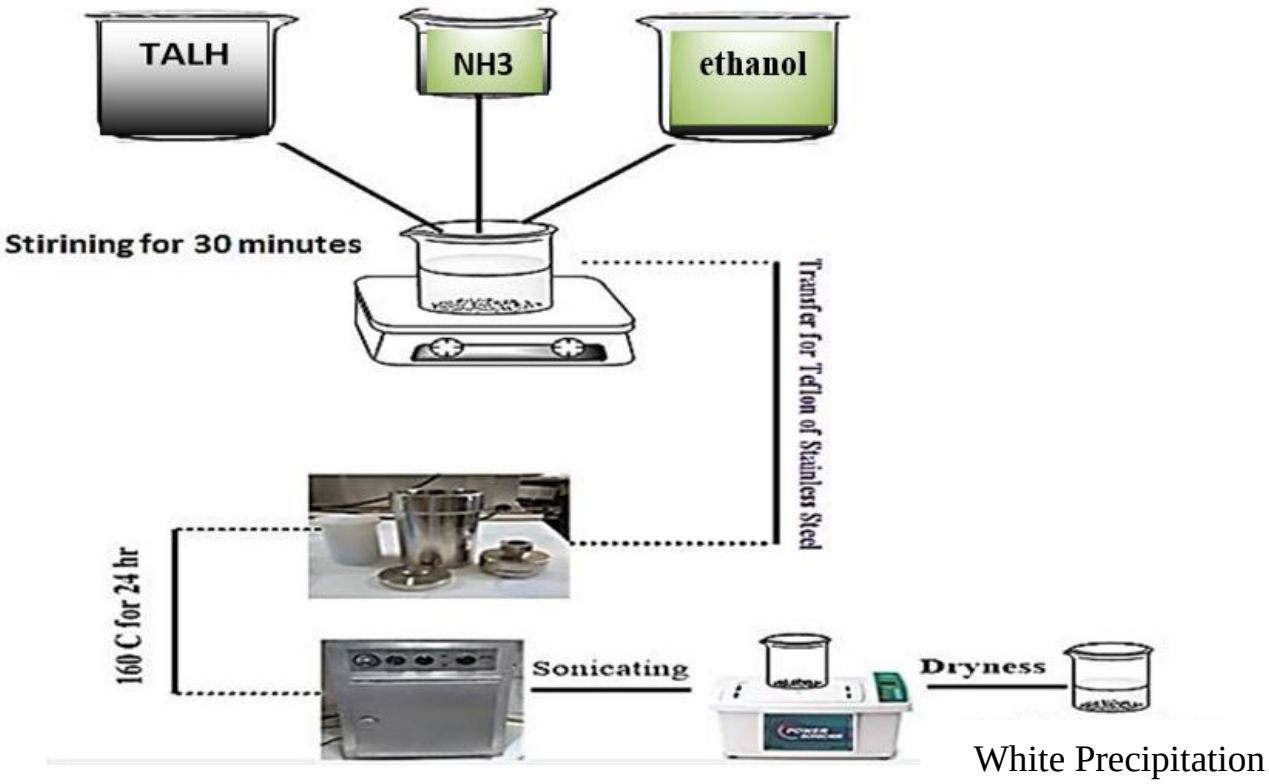

Figure(2-1) Scheme Preparation of TiO_2 Nanoparticle

2.4 Preparation of Silver (Ag) Doped TiO_2 Nanocomposites

The Ag deposited on TiO_2 Nano composite was prepared by placed 1g of TiO_2 NPs and 2.5 ml $AgNO_3$ (3 mM) in a quartz cell and added methanol and the

distilled water with ratio 1 % v/v (methanol /H_2O) and pargulated by N_2 (Nitrogen gas) for 10 minute, then the system was irradiated with UVA light(wavelength 365nm and light intensity of 1.71mW/cm^2) under continuous magnetic stirring for 10-12 h .After irradiation the resulted powder was washed several times with distilled water and dried 24 h in an oven at 60°C.Therefore we obtained Ag deposit TiO_2 , as appear in Figure (2-2) .

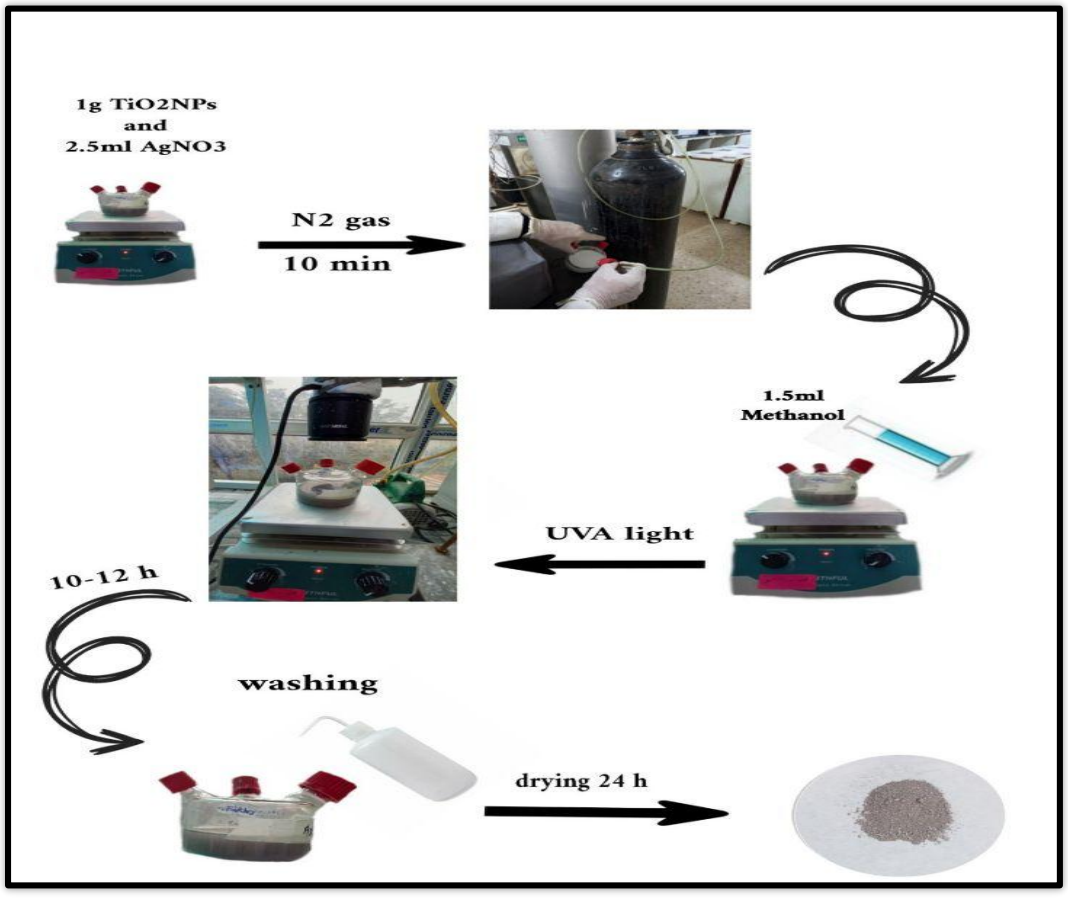

Figure(2-2) Scheme Real Image for Preparation of Ag/TiO_2 Nanocomposites

2.5 Characterization Techniques

Different techniques were used to characterize and study the structure and nature of Nano material . Thus, the common techniques were explained briefly in the following :

2.5.1 X-Ray Diffraction (XRD)

X-ray diffraction is a powerful nondestructive technique for characterizing crystalline materials. The crystalline properties of materials prepared using an X-ray deflection technique were studied using a single-wavelength light (0.15405nm) from the Cu-Kα source with the use of nickel as a filter. Where the range taken from deviation angles (2Θ) in this measurement is between (10-80) degrees.[76].

2.5.2 Field Emission- Scanning Electron Microscopy (FE-SEM)

FE-SEM is a powerful device that is used in characterizing sample morphology such as grain size, particle size, particle distribution, crystal defects and surface structure. FE-SEM has several features like large depth of field, higher resolution and more control in the degree of amplification. About 50μL of aqueous or ethanol suspension of sample was placed on a clean silicon wafer surface. Then dried at 80^{o}C to remove the solvent [77] .

2.5.3 Transmission Electron Microscopy (TEM)

TEM is a microscopy technique used a beam of electrons transmitted across an ultra-thin sample where the electrons are transformed into light and form an image and get magnification and hence details of the sample to much improved level that the conventional optical microscope reach to 1nm particle that can be also calculated. TEM produces numerous information of materials at including size distribution . morphology , crystal structure, TEM can be used in various

application such as research, science of nanotechnology and education .The TEM produce a 2D images with high resolution capacity[78].

2.5.4 Fourier-Transform Infrared Spectroscopy(FT-IR)

The vibrational motions of the chemically bound constituents of matter have frequencies in the infrared region. The oscillations induced by certain vibrational modes provide a means for the matter to couple with an impinge beam of infrared electromagnetic radiation and exchange energy with it when the frequencies are in resonance. Consequently, the molecular vibration will be excited by infrared frequency causing the energy of molecular vibration to increase. In the meantime, the electromagnetic radiation with a specific frequency will be absorbed by the molecule because the photon energy is transferred to excite molecular vibrations. FTIR spectra were recorded using the FTIR instrument (Shimadzu. 8400S) in the 4000-400 cm^{-1} frequency range. Dried absorbance (1 mg) was mixed with KBr powder (10 mg) in an agate mortar. The mixture was pressed into a pellet under 10 tons load for 2–4 min, and the spectrum was recorded and the spectrum was recorded immediately[79, 80].

2.5.5 Ultraviolet-Visible Spectroscopy (UV-Vis)

Ultraviolet-Visible spectroscopy is a method refers to absorption or reflectance spectroscopy through the regions of ultra violet and visible spectrum UV-Vis spectrum can be measured as an absorption / transmission spectrum . the wavelength range of UV from (100-400) nm can be consider shorter than the visible light (400-800) nm . It can be measures the intensity of light passing through the sample[81].

2.5.6 Thermal Gravimetric Analysis (TGA)

TGA is a powerful technique for the measurement of thermal stability of materials including polymers. In this method, changes in the weight of a specimen are measured while its temperature is being increased .Moisture and volatile contents of sample can be measured by TGA. The apparatus basically consist of a highly sensitive scale to measure weight change and a programmable furnace to control the heat up of the sample .A modern apparatus usually equipped with computer that can calculate the weight-loss fraction or percentage . A common application of TGA are determined organic and inorganic content in sample also material characteristic decomposition patterns[82].

2.5.7 Band Gap Energy Measurements

A semiconductor is a material that has low electrical conductivity at room temperature, but its conductivity increased by input of energy. The solid material composed of an inconceivable number of atoms and contains an infinite number of energy states. Because these energy levels are so closely spaced, they form bands instead of discrete energy states. This is the major difference between a solid material and a single molecule that contains a finite number of atoms and possesses discrete energy levels. The highest energy band that is filled with electrons is called the valence band. The next higher band that is empty is called the conduction band. The energy separation between these bands is called the band gap, Eg [83].

2.6 Photo Catalytic Degradation of Dye by Using Ag/TiO_2 Nanoparticles.

2.6.1 Determination of Optimum Wavelengths (λ max) of Malachite Green (MG) Dye

A Malachite green dye is a very well - known cationic dye that has a molecular formula ($C_{23}H_{25}ClN_2$), and molecular weight (364.9g/mol); the dye is odourless green crystals powder used for various purposes. A stock solution (1000 mg L^{-1}) was prepared by dissolving (1.0 g) of dye in (1000 mL) distilled water.

To determine the maximum wavelength of Malachite green dye the ultraviolet-visible absorption spectra of Malachite green dye solution was recorded within wavelengths of 200-800 nm. Where the maximum wavelength of the solution was determined from its highest absorption in the UV-Vis spectrum found at the wavelength λ_{max} MG= 624 nm in Figure (2-3).

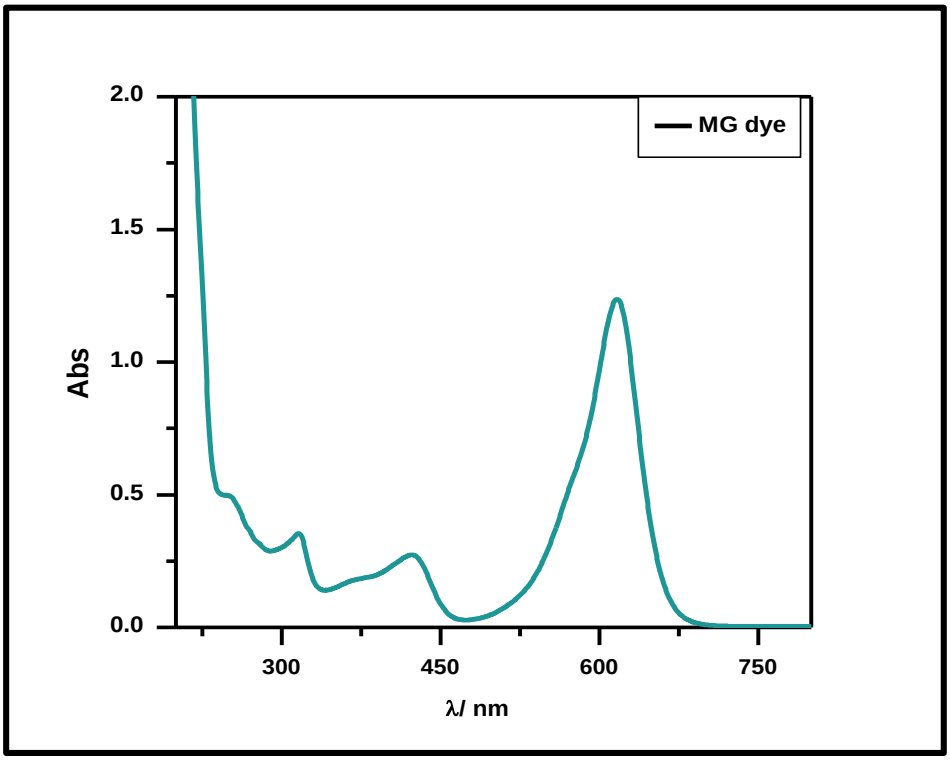

Figure(2-3): UV-Visible absorption spectra of Malachite green (MG) dye

2.7 Photo Catalysis Experiment

The photo catalytic of the Ag/TiO_2 nanoparticles catalyst was evaluated by the degradation of Malachite Green (MG) dye. All experiments were carried out in a photo- reaction vessel, the beaker was irradiated with the solar light maintaining the distance between the light source and the surface of the solution controlled by using UVA-meter. experimental tests were performed, 0.3 g Ag/TiO_2 photo catalyst was added into 200 mL solution MG dye. The mixture maintained in the dark for 10 min under stirring to reach adsorption equilibrium, and was then irradiated at different time intervals at 90 min. , as shown in Figure(2-4) . and separation the sample by centrifuged at 3500 rpm for 10 min .The concentration of MG dye was determined by measuring the absorption at its maximum absorbance wavelength of MG dye =624 nm, by using a UV-Vis spectrophotometer(UV mini-1240 Shimadzu, Japan) with 3 cm path length spectrometric quartz cell, and then calculated from calibration curve .Effect of various operational parameters such as amount of catalyst (0.1-0.4g/L) ,concentration of dye(25-150mg/L) , light intensity (1.72-2.96mW/cm^2) on the photo degradation efficiency was studied , while our studies depend on photo degradation efficiency were calculated using the following relationship

$$\text{PDE}\ (\%) = (C_0 - C_t)/C_0 \quad \text{x}\ 100 \quad \ldots\ldots\ldots\ldots (2-1)$$

Where, C_0 and C_t are the initial and photolysis concentration (mg/L), respectively, PDE (photo catalytic degradation efficiency), and t is time of irradiation (min.)

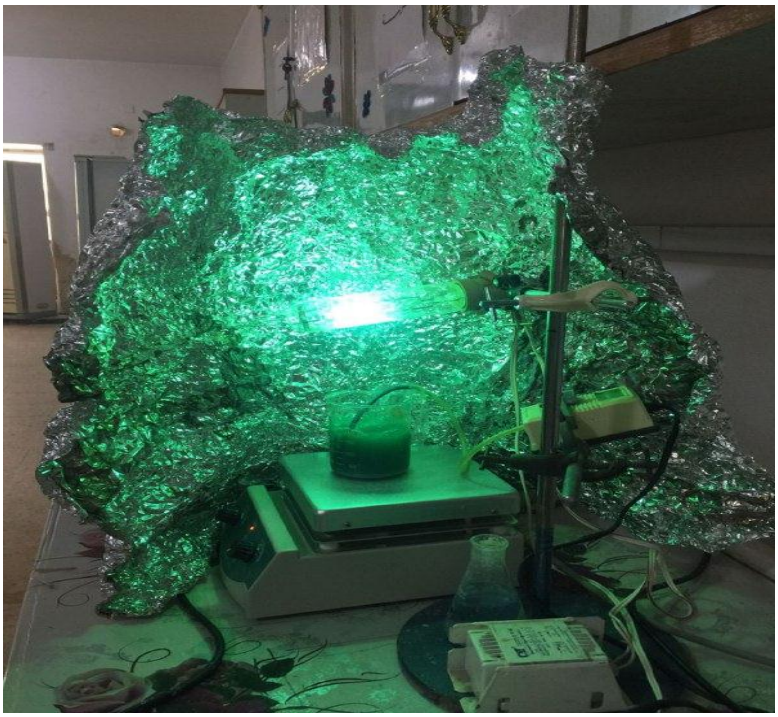

Figure (2-4): Real Image for the Experimental Photo Reaction

2.8 Experimental Design

The effect of the factors and their interactions were investigated from analysis of 3D-surfaces *via* RSM method. The design consisted of a full-factorial 2^3 (8 factorial points), 6 axial points and 4 replicates in the central point, totaling 18 experiments. The independent variables were evaluated in five coded levels: −1.68; −1; 0; +1 and +1.68. The independent variable ranges were chosen according to works published in the literature, which reported the experimental conditions used in the hydrothermal method to obtain TiO_2 and Ag/TiO_2 for the application[84].

Chapter Three

Results and Discussion

3.1Characterization of Titanium dioxide and Silver Nano composite

3.1.1 XRD Diffraction of TiO_2 and Ag/TiO_2 Nano composite

In **Figure.3-1** show the XRD patterns at of prepared TiO_2 and Ag-TiO_2 . In **Figure 3-1 (a)** the XRD pattern of TiO_2 there are no other summit indicate the presence of the impurity due to effect of calcination (500 ^oC), the diffraction peaks were observed at 25.3°, 37.9°, 48.2°, 54.5 °, 55.3°,62.02°and 68.7, which correspond to the (101), (108), (004), (112), (211), (200), (106) and (212) lattice planes of anatase TiO_2 (JCPDS card no. 21-1272) the crystal shape of the diffraction peaks appear clear and sharp[85, 86]

In Figure. 3-1(b) no crystalline phase involving Ag could be observed. This indicates that the Ag is too dispersed in the TiO_2 lattice is not sufficient for clear crystal formation or the Ag content is below the detection limit. Interestingly, no Ag crystal phase was detected. Thus, at low Ag content, higher dispersion of smaller Ag nanoparticles is on the surface and pores are clearly achieved.

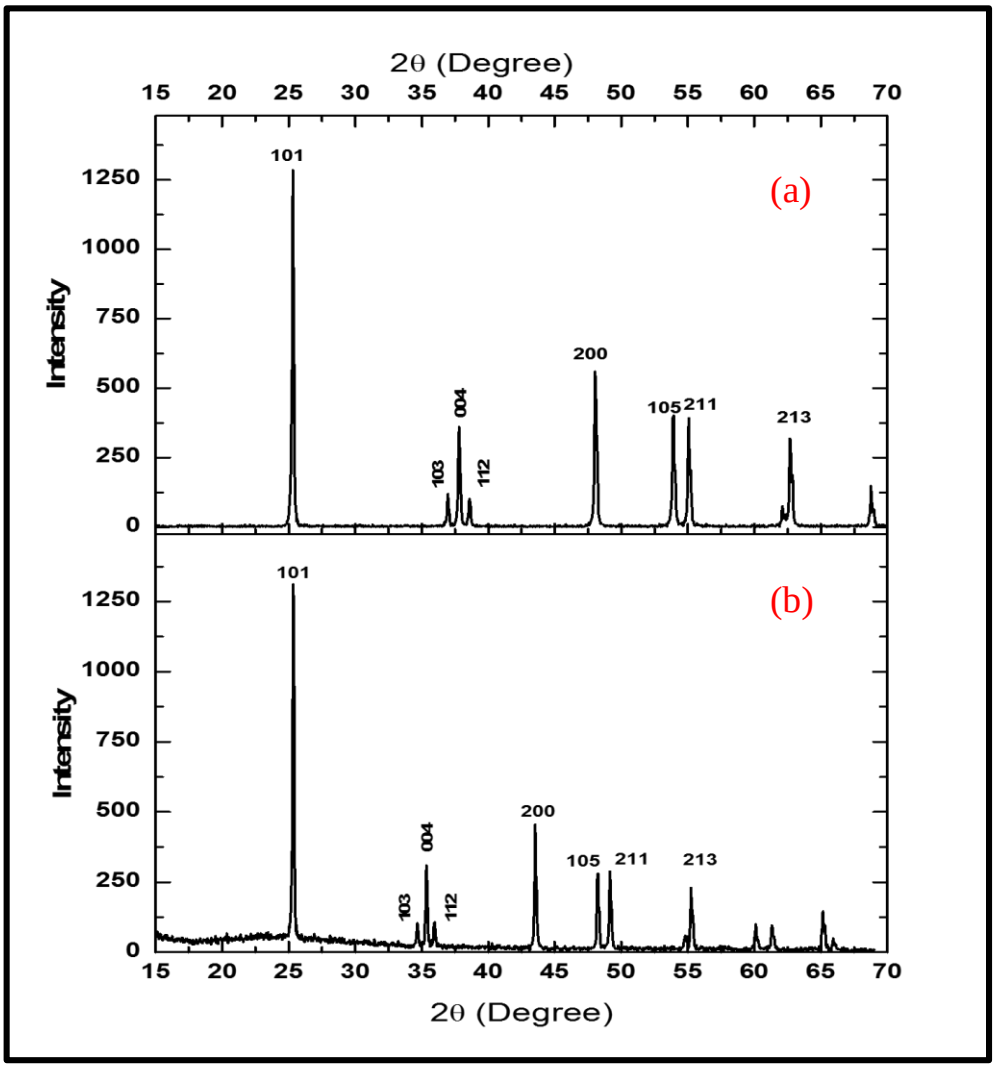

Figure (3-1): XRD Diffraction Patterns of (a) TiO_2 Nanoparticles and (b) Ag/TiO_2 Nano composite

3.1.2 FT-IR of TiO_2 and Ag/TiO_2 Nano composite

In Figure shows(3-2) a,b the FT-IR spectra of the preparedTiO_2 nanoparticles, and Ag/TiO_2 ,TiO_2 was clacinated at 500C° .The measurement was carried out at RT under air atmosphere.It is obvious from result that the absorption peak between (2344 and 2352)cm^{-1} is caused due to the existence of CO_2 molecule in air .It can be noted that the well resolved intense and broad transmission band below ≈≈ 500cm^{-1} was attributed to the stretching vibration Ti-O bond confirmed the

formation of TiO_2.A slight peak shift was observed at metal doping in the present study (between 500 and 485cm^{-1}) may be attributed to the change in particle size as a function of metal doping .All these vibrational modes present in the sample confirm the formation of TiO_2 Nano structure [87, 88]

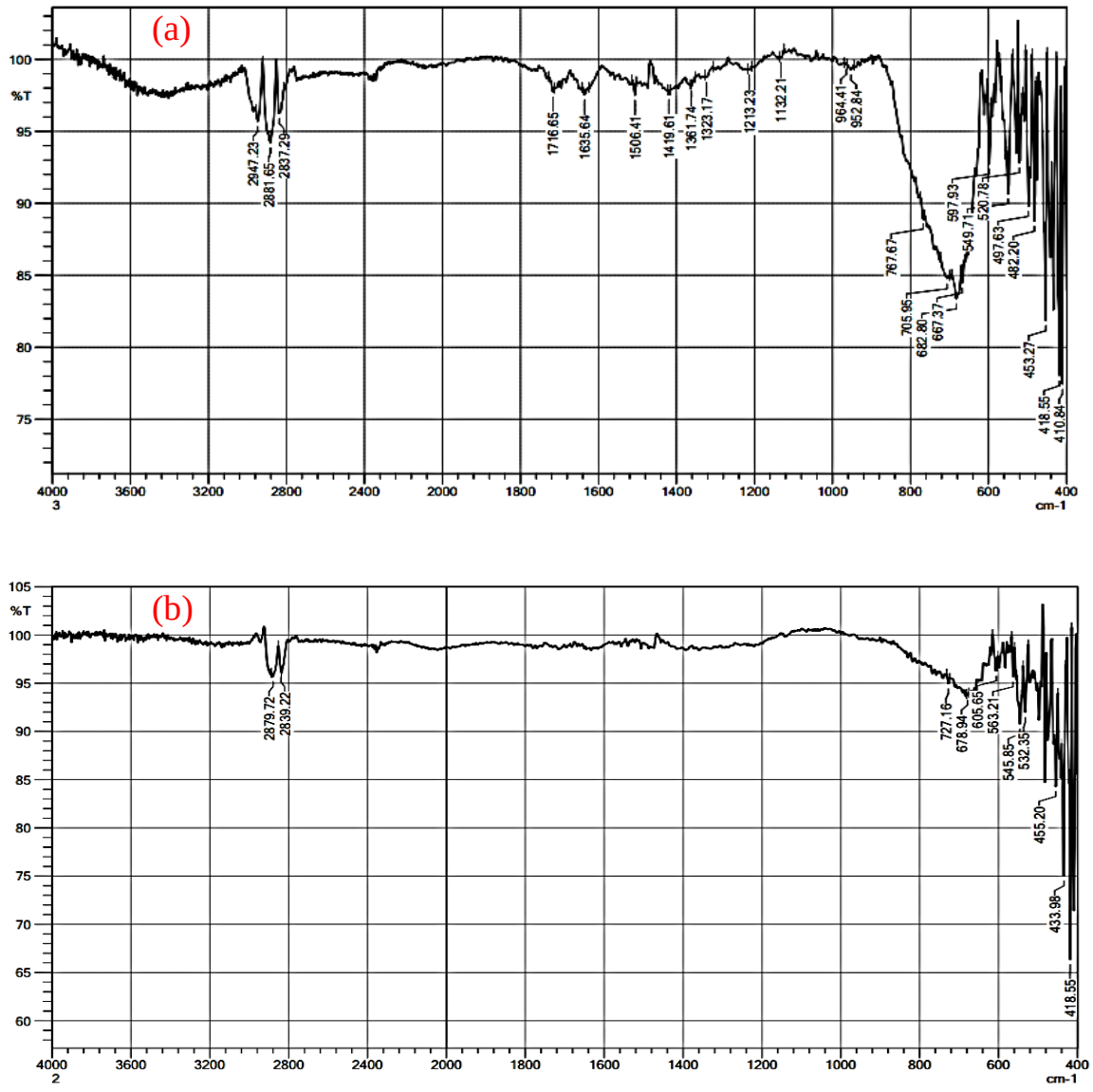

Figure (3-2) FT-IR Spectra of (a) TiO_2 Nanoparticle and (b) Ag/TiO_2 Nano composite

3.1.3 TGA of TiO_2 and Ag/TiO_2 Nano composite

Thermo gravimetric analysis (TGA)technique in which the mass of a sample is monitored against temperature or time, to study the thermal stability of Nano composite and indicate the purity of nanocomposites, the TGA curve of (a TiO_2 NPs and b) Ag/TiO_2 Nano composite in the temperature range 100- 600 °C Figure . the TGA curve of TiO_2 NPs and also curve Ag/TiO_2 Nano composite appear straight line due to thermal stability.

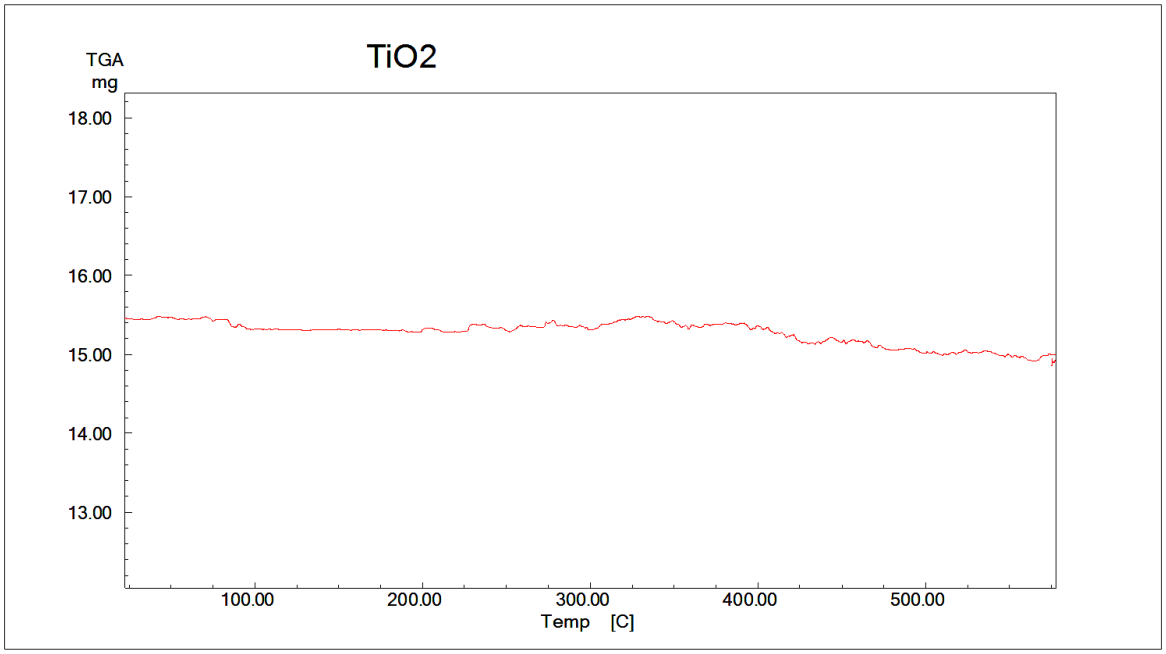

Figure (3-3) TGA Curve of TiO_2 Nanoparticle

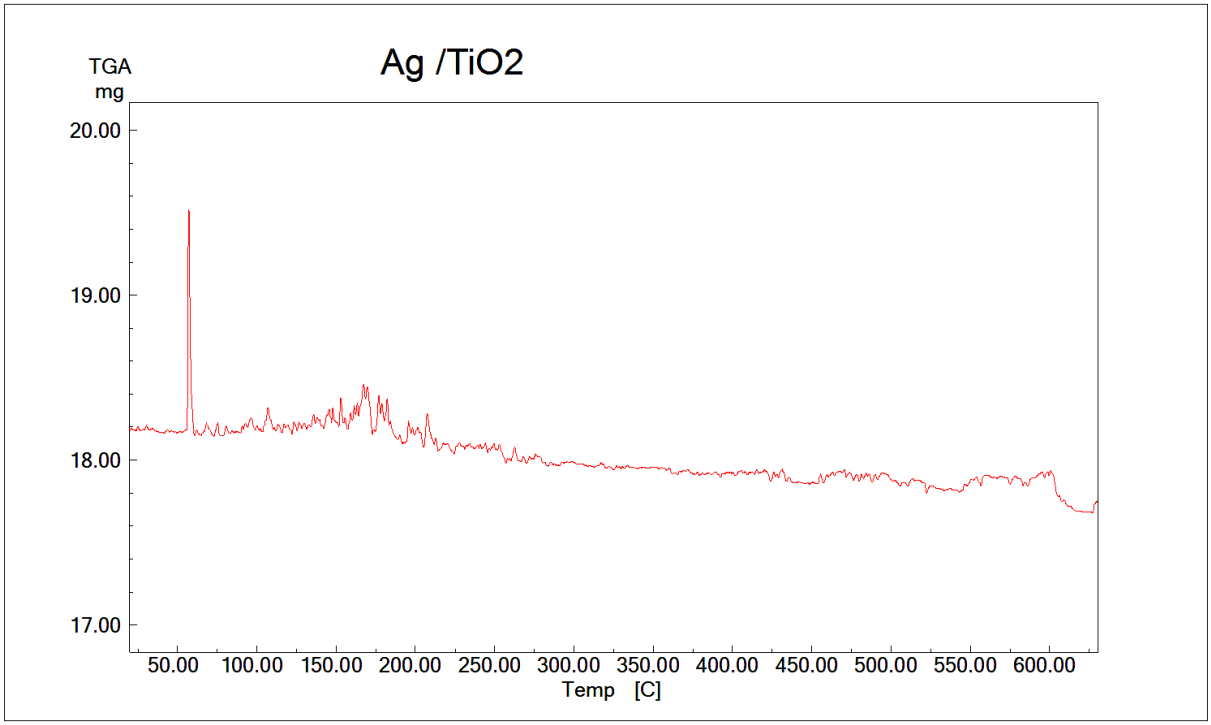

Figure (3-4) TGA Curve of Ag/TiO_2 Nano composite

3.1.4 FE-SEM Image of TiO_2 and Ag/TiO_2 Nano composite

The surface morphology of pure TiO_2 nanoparticles has been studied in terms of the size, shape of particles and clusters among them, in addition to the distribution of these particles using the SEM technique. Figure. 3-5 shows SEM image of TiO_2, the nanoparticles have anatase shape with a mean size of between (29.34-41.34) nm with highly of agglomerate.

Silver nanocomposites were found to be overlapped with TiO_2 nanocomposites which exhibits cubic like morphology and their particle size ranges from around (48.34-120) nm as shown in Figure(3-6).

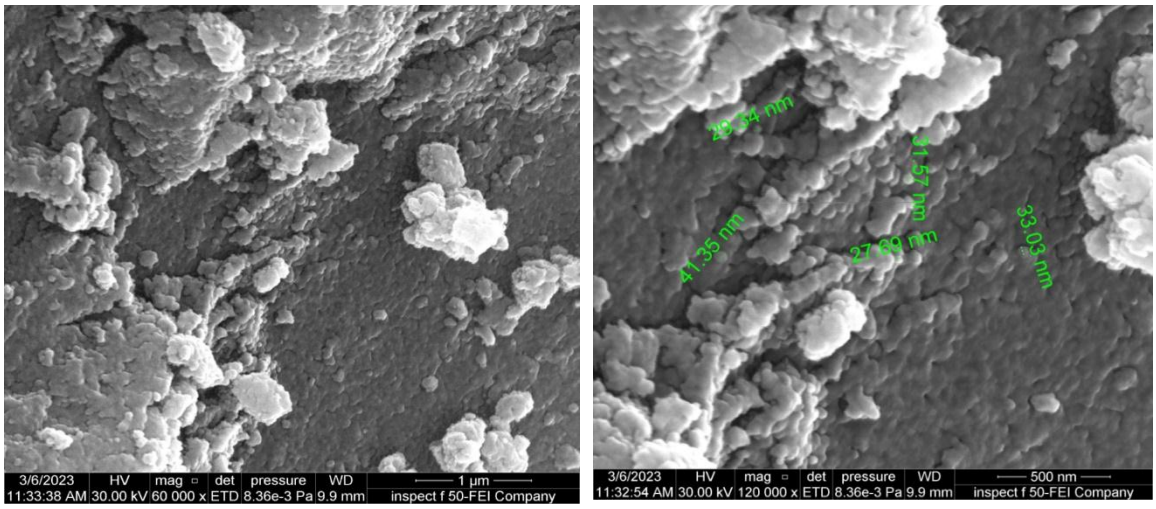

Figure (3-5) FE-SEM Image TiO_2 Nanoparticle

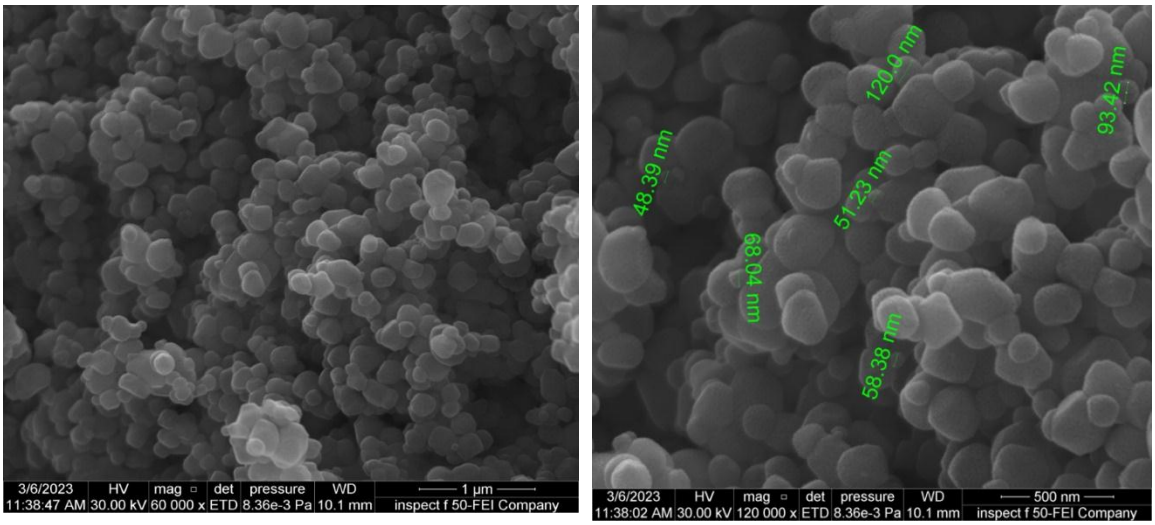

Figure (3-6) FE-SEM Images of Ag/TiO_2 Nano composite

3.1.5 Energy Dispersion X-ray (EDX) Analysis of Ag/TiO_2 Nano composites:

EDX examination provides information on chemical composition of sample. Figure shows that the prepared sample is mainly composed of Ti and O with small amount of Ag.

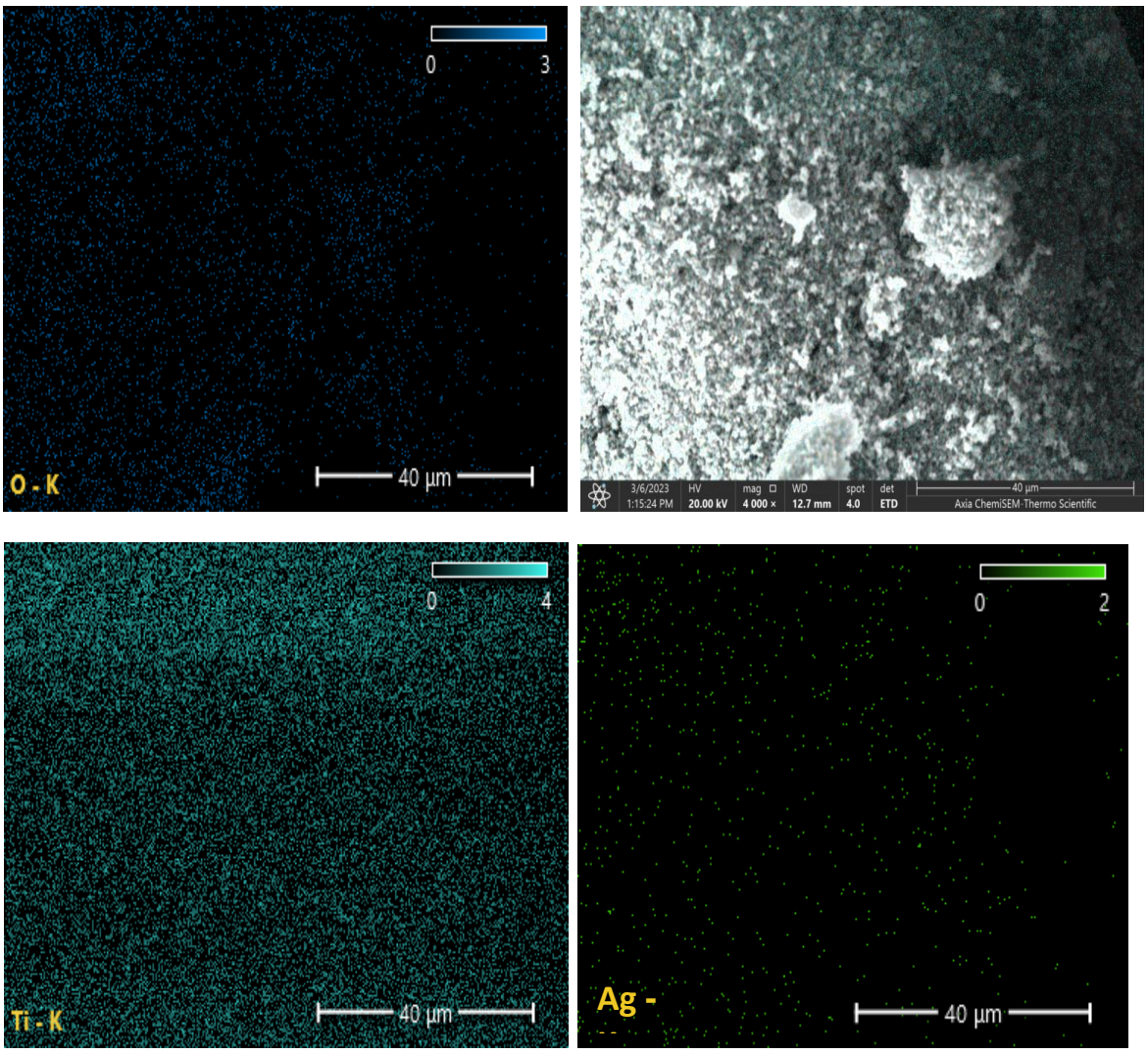

Figure (3-7) EDX Analysis of Ag/TiO_2 Nano composite

3.1.6 TEM of TiO_2 Nano particle and Ag/TiO_2 Nano composite

The transmission electron microscopy gives a more accurate picture of the structure of prepared samples ; the crystalline, distribution and the particles size of nanocomposites is shown in Figure(3-8) a . The TEM image shows that of TiO_2 NPs appears in the form of cluster inside the surface with needle shape. The micrographs of Ag/TiO_2 as shown in Figure(3-8) b Ag Nano particles were clearly observed in the TEM images as the most intense dark spots on the TiO_2 surface .The Ag Nano particles deposited on the TiO_2 are quite small and well deposit on the TiO_2.

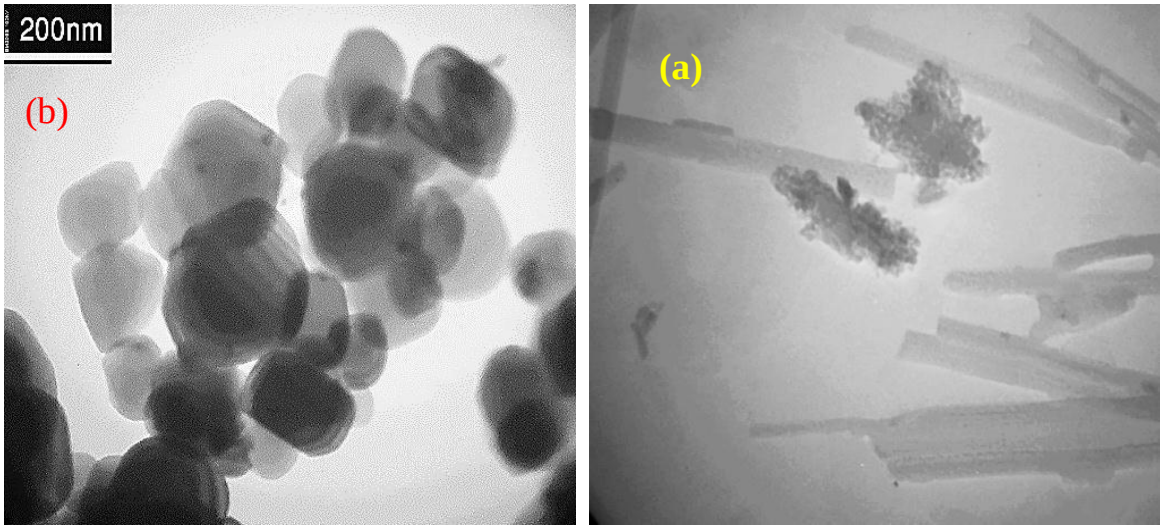

Figure (3-8) (a) TEM of Image TiO_2 Nano particle and (b) TEM image of Ag/TiO_2 Nano composite

3.1.7 UV -Vis Diffuse Reflectance Measurement

The quantity of the energy band gap of prepared Nano composites has been determined by studies of optical properties of these particles using UV-Vis Spectroscopy in the range of wavelengths 300-700 nm .The band gap energy was calculated based on the absorption spectrum of the sample according to the following equation:

$$E_{bg} = 1239.8/\lambda g \qquad (3\text{-}1)$$

Where, E_{bg} is The band gap energy of the photo catalytic, λg is the wavelength in nm used the absorption edge. Also the band gap of Nano composites can be calculated by Tauc's plot which is expressed as follows

$$(\alpha\, h\nu)^{1/n} = A\,(h\nu - E_{bg}) \qquad (3\text{-}2)$$

Where α is the absorption coefficient, h is Planck's constant, ν is frequency ($\nu = c/\lambda$, c light speed, λ is the wavelength). n = ½, 2 for direct and indirect band gap, respectively. A is proportionality constant, and E_{bg} is band gap[89, 90]

The results for pure TiO_2 in Figure(3-9) shows shifted with black colour and no absorption in visible range with strong UV absorption at 380 nm, the calculated band gap of TiO_2 nanoparticles was found to be 3.23 eV .This indicates that the TiO_2 is related to the anatase structure of TiO_2 crystal and may be due to change transfer band from O:2p to Ti:3d [91, 92]

In metal nanoparticles such as in silver nanoparticles influence the band gap of the Nano composite by creating of trap levels for electrons between the conduction bands and valence bands of TiO_2. The loading of Ag nanoparticles on

TiO_2 results in the synergetic interaction of the Ag nanoparticles on the TiO_2 surface, surface Plasmon resonance effect, reduction of the band gap, and enhancement of the charge transfer . [93, 94] According to the results, the band gap slowly decreases with the increase of the Ag doping TiO_2 and small change was observed as shown in Figure(3-9) .

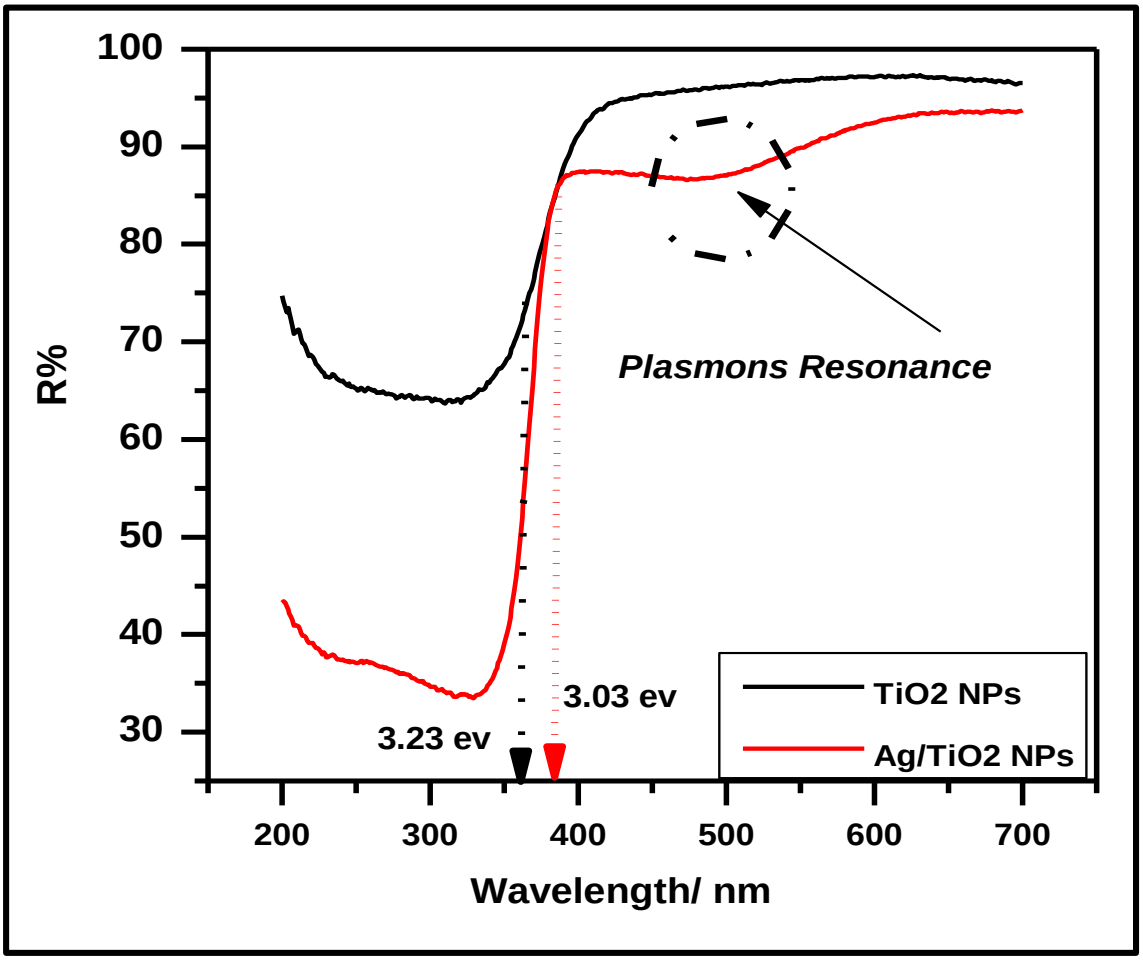

Figure (3-9):Diffuse Spectra of TiO_2 Nano particles and Ag/TiO_2 Nano composites

3.2 Application of Prepared Nano composite

3.2.1 Effect of Ag/TiO_2 NPs Dosage

The influence of the photo catalyst concentration (0.1-0.4g/L) on the photo catalytic degradation of MG dye was investigated at an initial malachite green(MG) dye concentration of 50 mg /L, light intensity (2.1 $mW.cm^{-2}$), flow rate of O_2 (5mL/min) and pH 8.1 .In the regain less than 0.4 g/L when the mass dosage were increased , the rate of degradation was increased because the number of active sites increase[95] as Figure(3-10). This shows that the precent degradation of modified catalyst increase with increase in the amount of catalyst from 0.1 - 0.4 g/L and above this limit is not much change . This indicate that the active site provided for the adsorption of substrate on the catalyst surface is limited to catalyst amount of 0.3g/L and after that low change in the degradation . At higher dosage vacant sites are consumed by the intermediate products obtained during the reactions which retard further degradation of the substrate .Hence the percent degradation decreased or retained without notice change, the results of the change in percentage photocatalytic degradation efficiency (PDE%) with concentration of Ag/TiO_2 as Figure(3-11[96, 97]

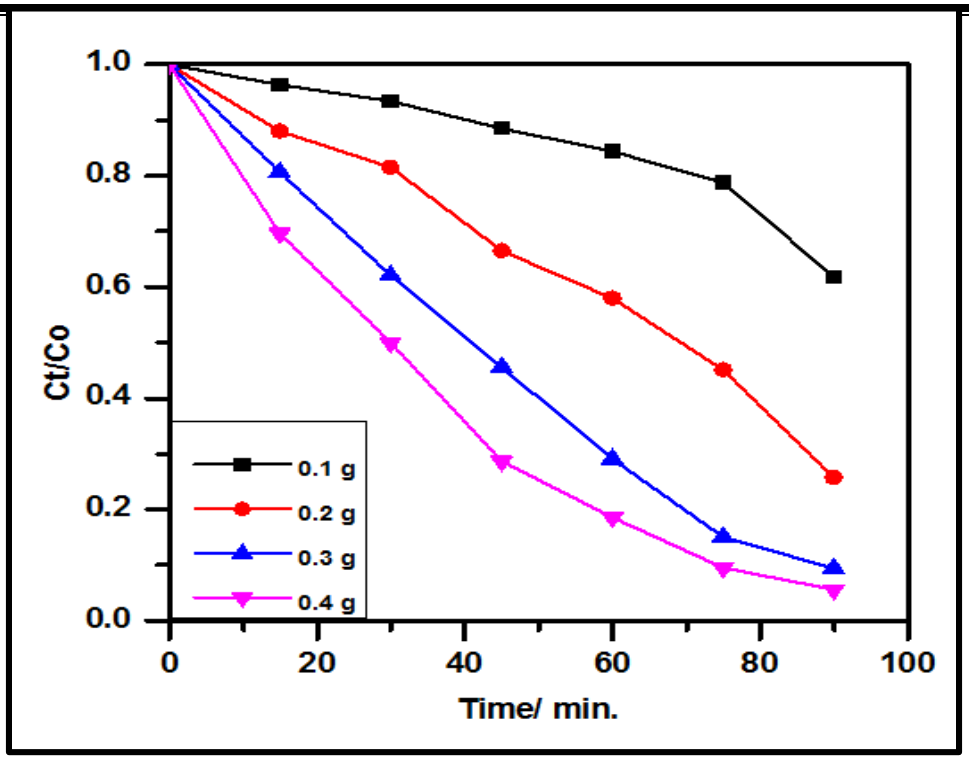

Figure (3-10): Photo Catalytic Degradation of Malachite Green , at Different Amount of Ag/TiO_2

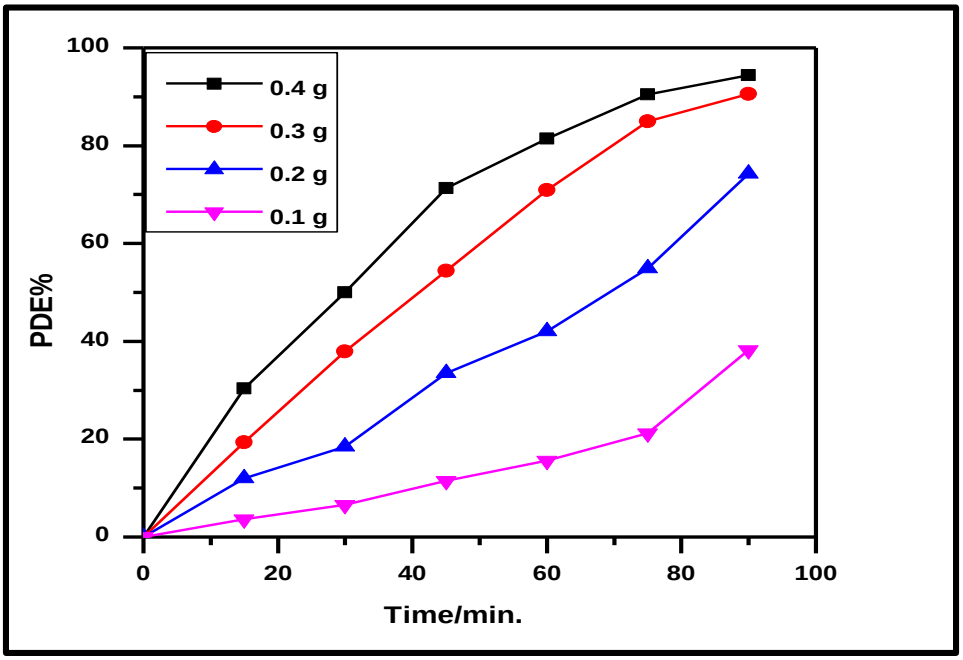

Figure(3-11) : Effect of Amount of Ag/TiO_2 on the Photo Catalytic Degradation of Malachite Green Dye

3.2.2 Effect of Malachite Green (MG) Dye Concentration

The effect of change initial (25-150 mg/L) on photo catalytic degradation process of malachite green dye was studied using 0.3g/L . The light intensity equal to (2.1mW.cm^{-2}) and temperature 25C$^{\circ}$. The results are plotted in Figure(3-12), it has been observed that the rate of photo catalytic degradation gradually decreases with increasing of initial malachite green dye concentration[98] , this behavior could be explained the concentration 50 mg/L was the optimum concentration to over largest area of the Ag/TiO_2 Nano composite, therefore absorbed maximum exciting photons to generate higher concentration of the activated Ag/TiO_2 Nano composite ,the concentrated solution becomes more intense in color which result in hindrance to penetration of radiation to the catalyst surface also, the ratio number of OH radicals to number of molecule of dye decrease in concentration , therefore decrease the photo degradation but the concentration of MG dye 50mg/L gives the optimum photo catalytic degradation efficiency which is 100% .The results of the change in percentage photo catalytic degradation efficiency with concentration of MG dye plotted in Figure (3-13)[96, 99]

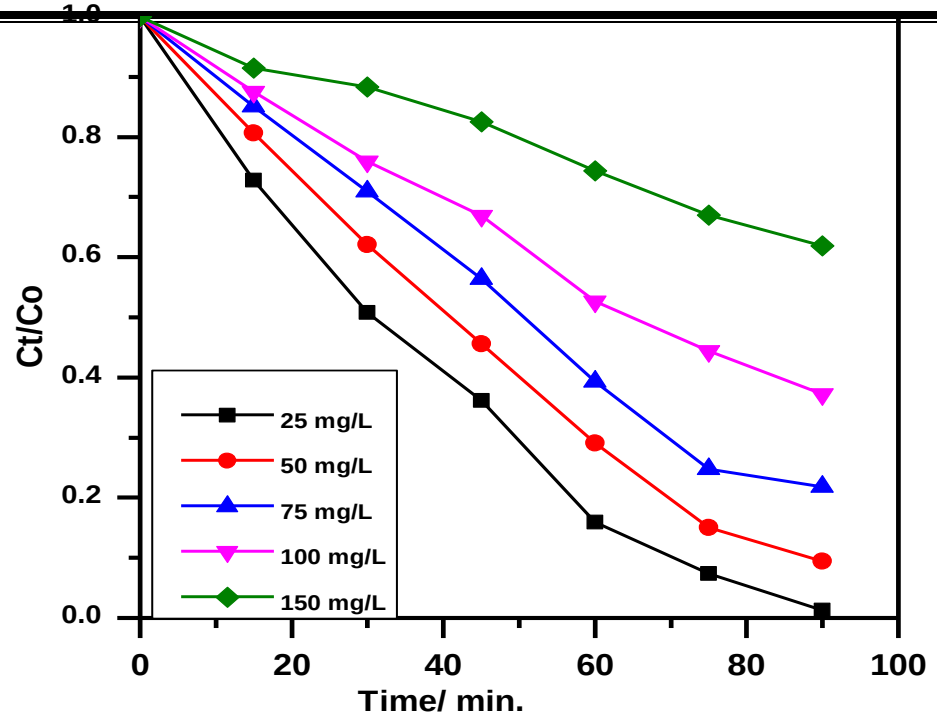

Figure (3-12): Photo Catalytic Degradation of Malachite Green at Different Initial Concentration

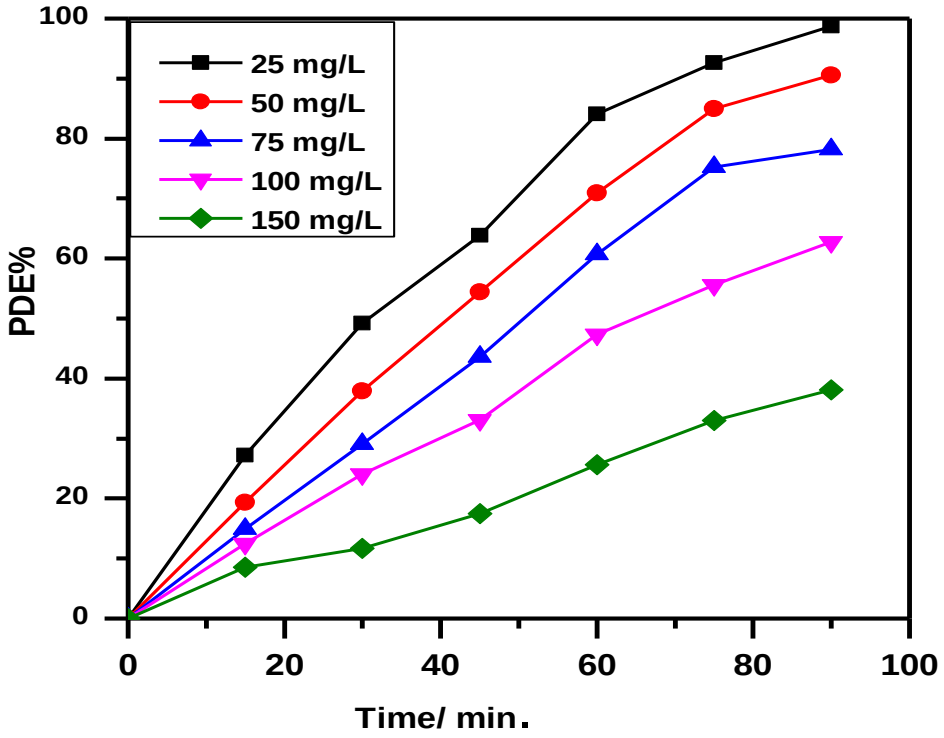

Figure (3-13): Effect of Initial Dye concentration on the Photo Catalytic Degradation of Malachite Green Dye

3.2.3 Effect of Light Intensity (L.I.)

The effect of light intensity about (1.72-2.96 $mW.cm^{-2}$) was observed via variable of distance between light source and exposed surface (Ag/TiO_2) Nano composite. Malachite green dye photo degradation via the effect of light intensity was investigation in the presence of 0.3 g/L of Ag/TiO_2 Nano composite, concentration of MG dye 50 mg/L . It was that found wholly reactions still follow the first order kinetics as appear in Figure (3-14) When light intensity was increased photo catalytic degradation was increased. It probably deduced, the rise of light intensity caused to excited particles of Ag/TiO_2 Nano composite to lead electron- hole pairs and photo degradation efficiency decrease when at low light intensity because of low light intensity reactions involving formation electron-hole are predominant and electron- hole recombination is negligible [100, 101], as shown in Figure (3-15).

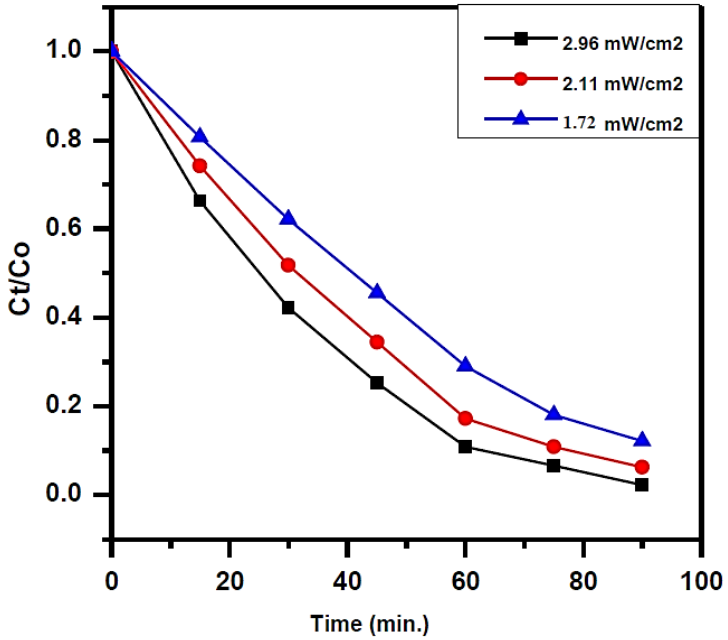

Figure (3-14): Photo Catalytic Degradation of Malachite Green Dye at Different Light Intensities

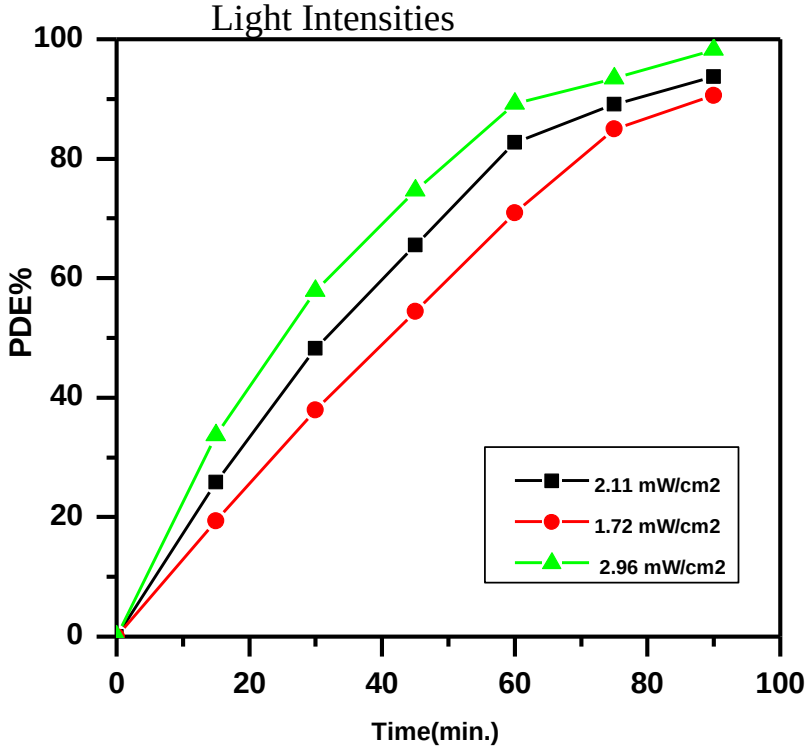

Figure (3-15): Effect of Light Intensity on the Photocatalytic Degradation of Malachite Green Dye

3.2.4 Recycling of the Photo Catalyst Ag/TiO_2 NPs

The recycling of catalyst is one of the key steps in assessing the practical application of photo catalysts and in developing heterogeneous photo catalysis technology for wastewater treatment. In Figure (3-16)An examination of the photo catalytic activity of the recycled Ag/TiO_2 NPs catalyst was carried out on malachite green dye. The photo catalytic degradation efficiency under experimental test(0.3g/L amount of dosage, initial malachite green dye concentration 50 mg/L, light intensity 2.1mW.cm^{-2}) which found that 83.9% ,78.8% ,and 68.5% during 3 cycle compared to standard solution(fresh) was 90.9% as show in Figure (3-17) .The result reveal of photo catalysts has self – clean property and reuse ability which makes it effective ,and thus the photo catalyst is basically stable and is therefore promising for environmental remediation[102] .

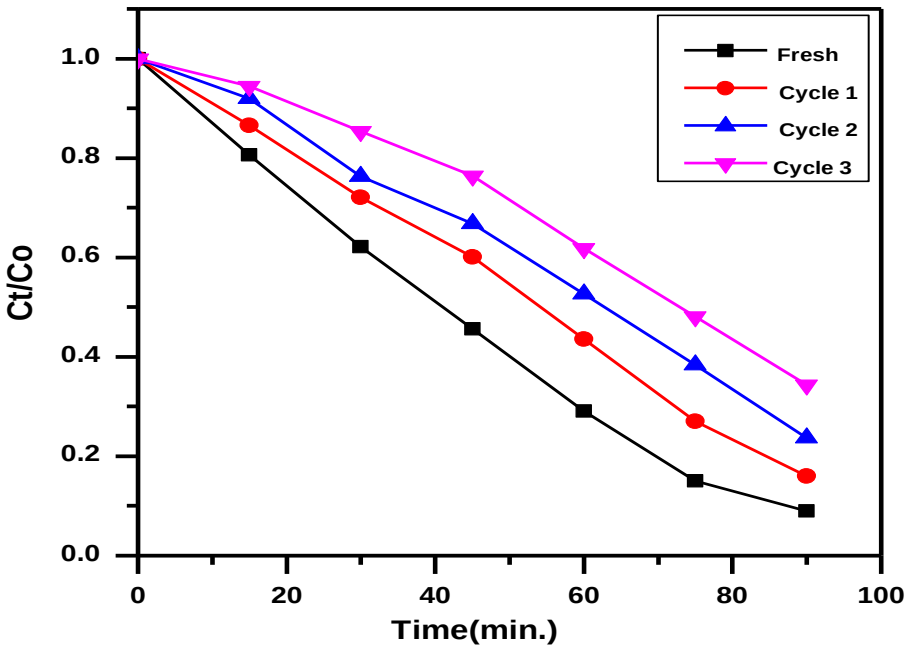

Figure (3-16): Effect of Recycling of Ag/TiO_2 Nanoparticle on Photocatalytic Degradation of Malachite Green Dye,Experimental condition :mass amount 0.3g/L dye of concentration 50 mg/L ,Light Intensity 2.1mW/cm^2

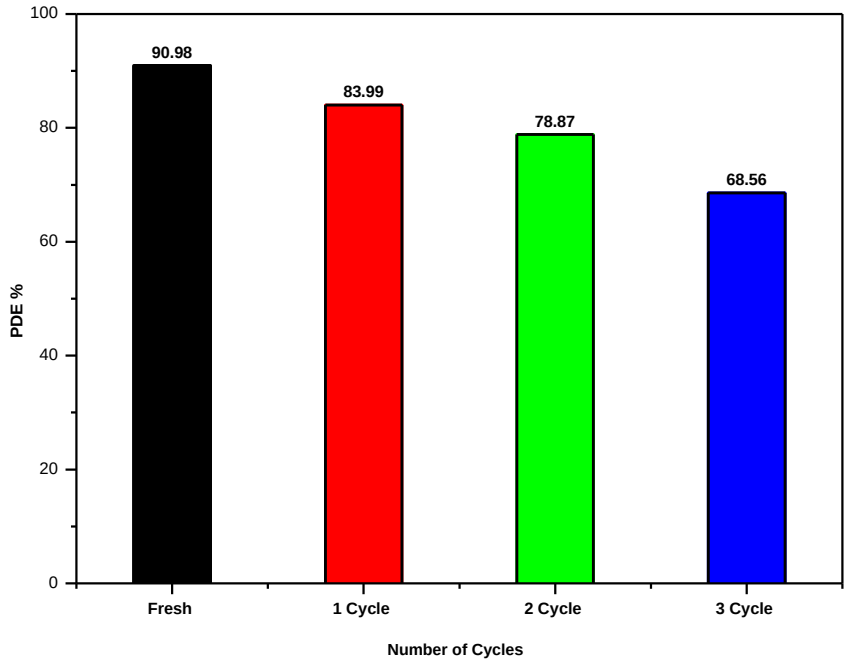

Figure (3-17) Reusability of the Photo Catalyst for Photo Catalytic Degradation Malachite Green Dye

3.2.5 Roles of Reactive Oxygen Species (ROS)

In order to distinguish the contribution of the surface reaction with(OH • ,O2 -• ,H_2O_2) species, different ROS were employed for check their effects on the relative photonic efficiencies of MG dye. The reaction pathway of MG degradation through generation of radicals from photo generated electron-hole pairs (e - CB; h + VB) .Hydroxyl radicals and electrons and holes (e - CB; h + VB) have an affected on photo catalytic degradation process[103] The recombination lifetime of the photo generated electrons and holes and the interfacial electron-transfer rate were used to determine the overall quantum efficiency of photo catalysis. To strengthen the quantum efficiency, the most general way is to try to retard the

recombination of photo generated holes and electrons. Therefore, filling the valence band holes by the electrons of some kind of reductant may confirm the photocatalytic for 60 min. as shown in Figure (3-18) when methanol was added, the photo catalytic degradation changed and reduced indicating that H_2O_2 can be important in the photo catalytic , while Figure (3-19) shows that degradation efficiency between H_2O_2 and Methanol**.**

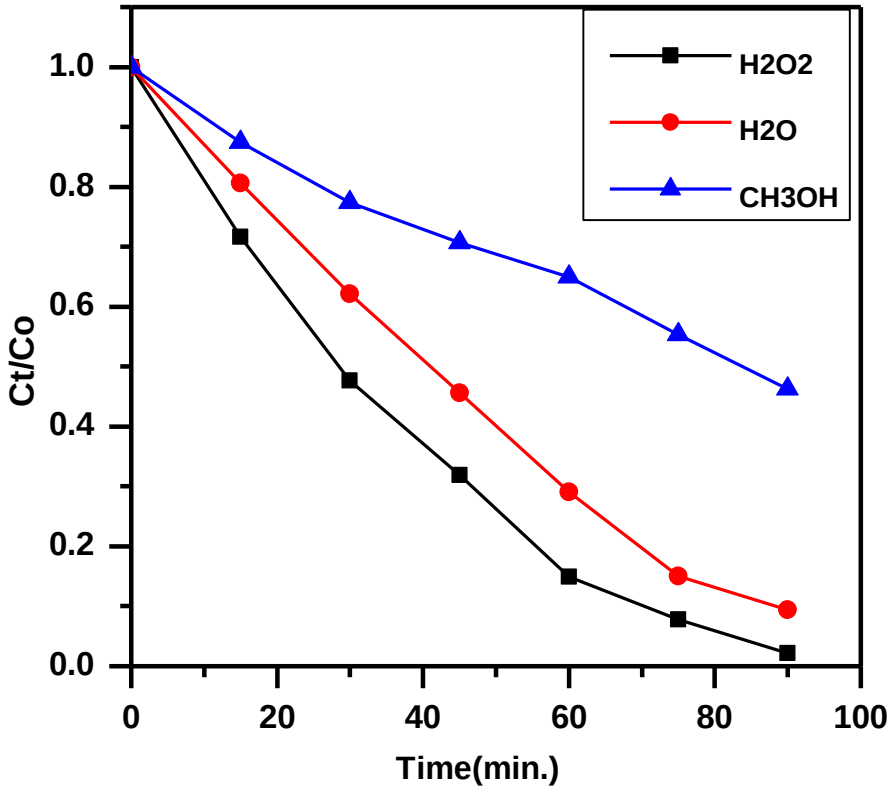

Figure (3-18): Effect of H_2O_2 and CH_3OH on Photo Catalytic Degradation of Malachite Green Dye, Experimental Condition :Mass Amount 0.3g/L ,MG Concentration 50mg/L ,Temp. 25C° , Light Intensity 2.1mW.cm^{-2}

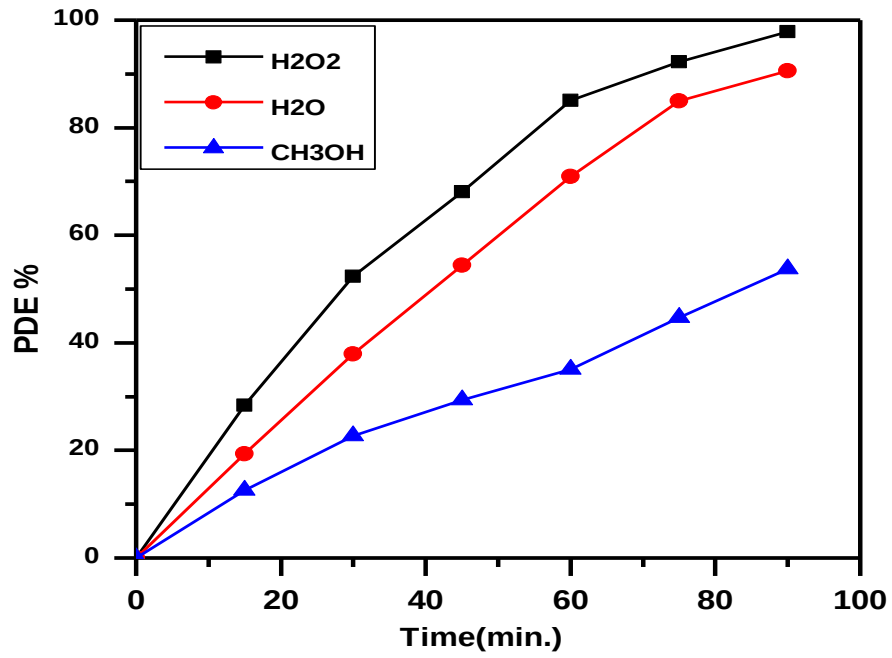

Figure (3-19) Effect of Degradation Efficiency between H_2O_2 and CH_3 OH on the Malachite Green Dye, Experimental Conditions: Catalyst Loading 0.3 g/L , MG Concentration 50mg/L , Light Intensity 2.1mW/cm^2

3.2.6 Removal of Pollutants (Mixture of Dyes) by Using Ag/TiO_2 Nanoparticles

A laboratory sample 200 mL of dye pollutants containing Brilliant Green(BG) , Congo red (CR), Methyl Violet (MV), Malachite green (MG), Methylene Blue (MB) , Brilliant Blue (BB) , Direct yellow (DY) and Reactive blue (RB) with a refry concentration were using in this study, then added to beakers in the presence of 0.3 g from prepared Ag/TiO_2 Nano particle., after that the mixture of beaker was put under the ultra violet light maintaining the distance between the light source and the surface of the solution controlled by using UVA-visible meter .The period was recorded under UV light for 2 h, after that centrifugation at 3500 rpm, and measured the remaining concentration by using

UV-Visible spectrophotometer at chosen wavelength at 530 nm , show in Figure (3-20) and found when time increase the absorption decrease and gave higher percentage removal .

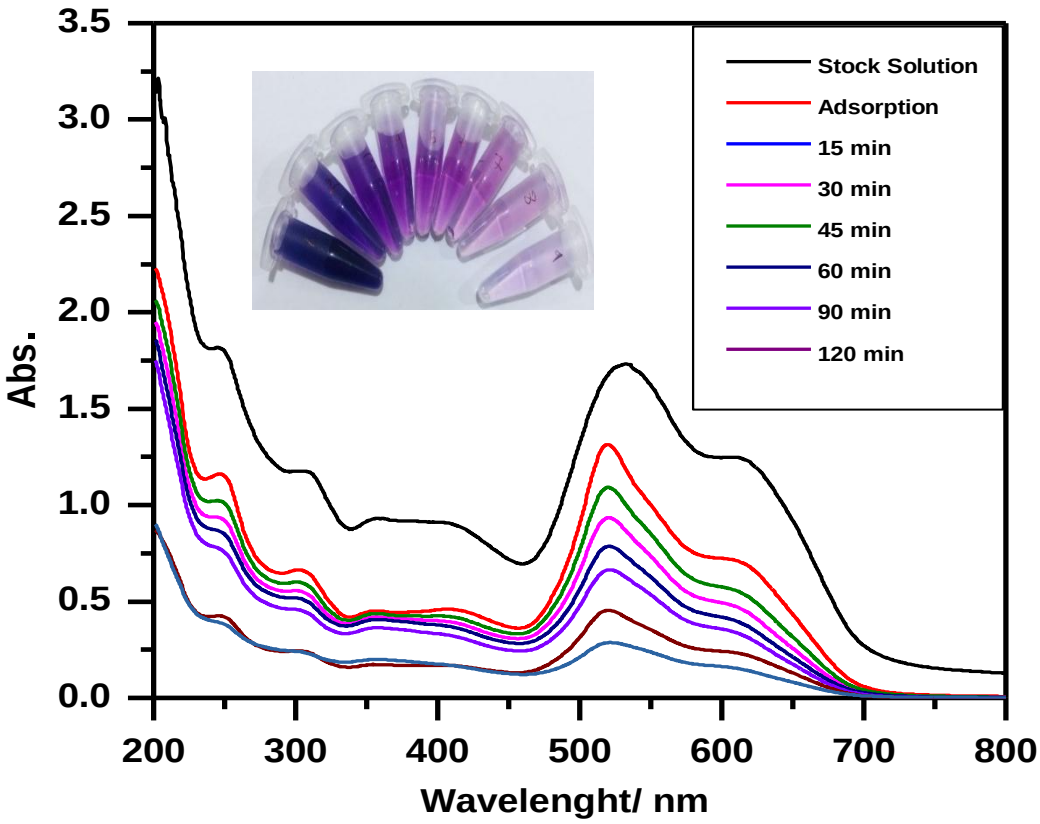

Figure(3-20) Effect Removal of Real Sample(Mixture of Dyes) by using Ag/TiO_2 NPs , Experimental Condition: Mass Amount 0.3g/L, Initial Concentration 50mg/L, Temp.25C° and Light Intensity 2.1mW.cm^{-2}

3.3 Response Surface Methodology (RSM)

The experimental design and k_{app} values of GRL photo degradation kinetics, using the different materials obtained *via* TiO2 surface prepared by Hydrothermal method are shown in Table 3-1.

Table (3-1) Central Composite Rotatory Design and Values of Apparent Photo Degradation Rate Constant

Run	L. I.	Conc. ppm	Amount of catalyst g/200 ml	Time / min	P. D. E.%
1	1.72	50	0.1	15	3.61
2	1.72	50	0.1	45	11.44
3	1.72	50	0.1	90	38.11
4	1.72	50	0.2	15	19.37
5	1.72	50	0.2	45	54.43
6	1.72	50	0.2	90	74.23
7	1.72	50	0.3	15	30.01
8	1.72	50	0.3	45	71.04
9	1.72	50	0.3	90	94.38
10	1.72	50	0.4	15	19.37
11	1.72	50	0.4	45	54.33
12	1.72	50	0.4	90	90.58
13	2.11	50	0.3	15	25.86
14	2.11	50	0.3	45	65.51
15	2.11	50	0.3	90	93.67
16	2.96	50	0.3	15	33.73
17	2.96	50	0.3	45	74.69
18	2.96	50	0.3	90	95.78
19	1.72	25	0.3	15	27.23
20	1.72	25	0.3	45	63.86
21	1.72	25	0.3	90	98.99
22	1.72	75	0.3	15	14.95
23	1.72	75	0.3	45	43.58

Run	L. I.	Conc. ppm	Amount of catalyst g/200 ml	Time / min	P. D. E.%
24	1.72	75	0.3	90	78.02
25	1.72	100	0.3	15	12.49
26	1.72	100	0.3	45	33.04
27	1.72	100	0.3	90	62.74
28	1.72	150	0.3	15	8.59
29	1.72	150	0.3	45	17.53
30	1.72	150	0.3	90	38.14

Figures below shows the 3D-surfaces, while this Figures displays the contour response surfaces for response k_{app} as a function of two factors, maintaining the third at its central level. It can be seen in Figure(3-21), the surfaces showed convex profiles with the highest k_{app} values being found near the central points (x_1 = 2.34 mw/cm2; and x_2 = 87.5 mol/l).

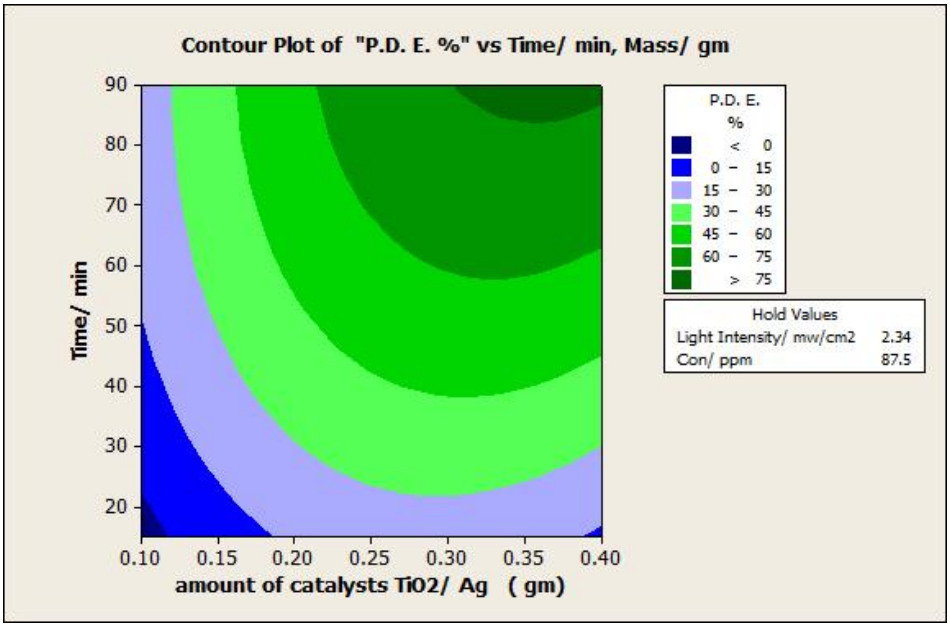

Figure(3-21): Contour Plot P.D.E. % Irradiation Time vs Mass of Catalyst

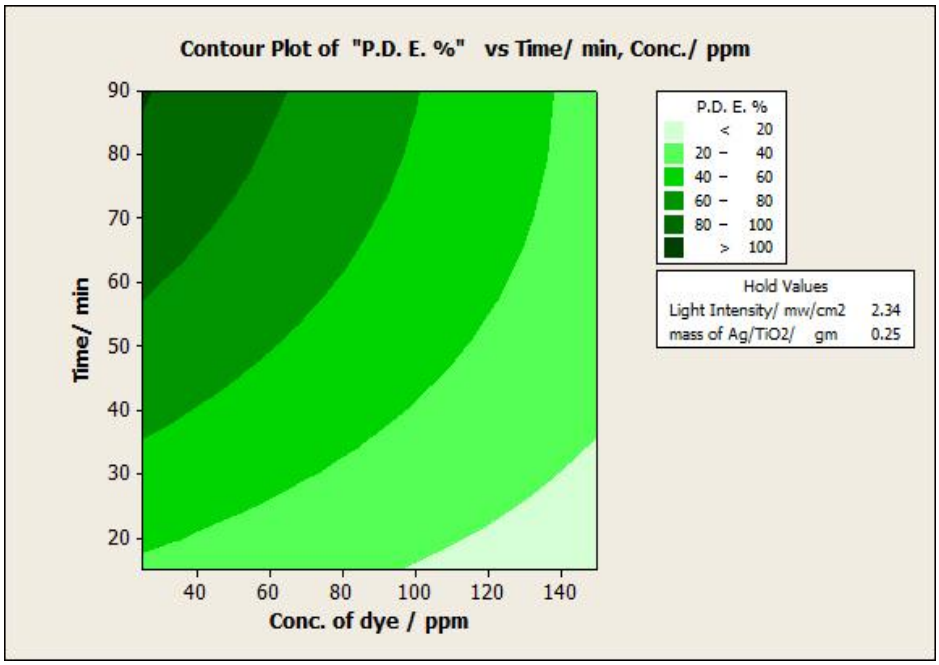

Figure(3-22):Counter Plot of P.D.E. % Irradiation Time vs Concentration of Dyes

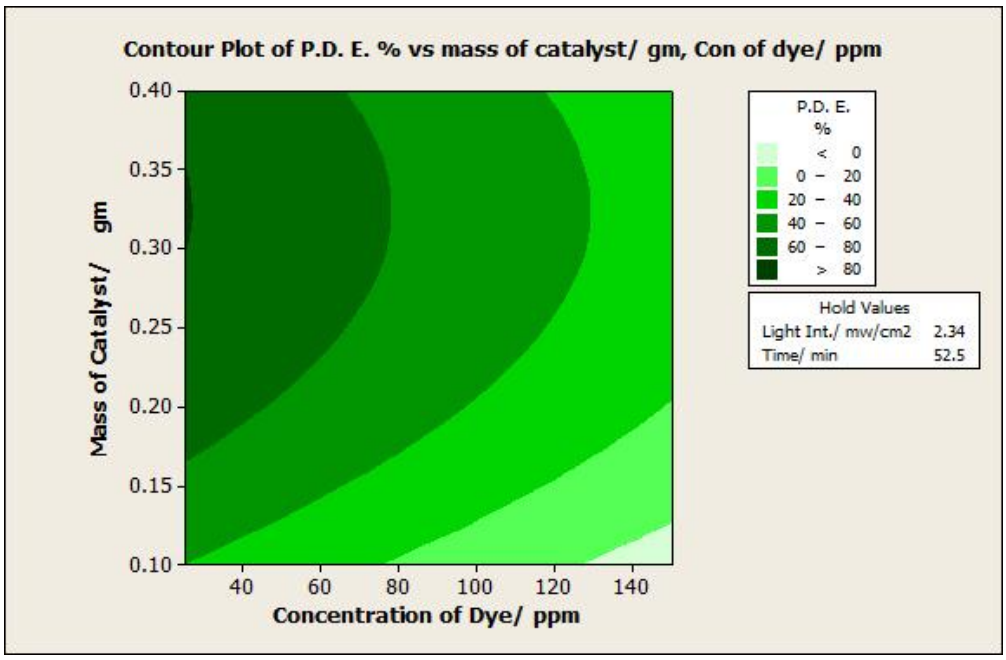

Figure(3-23): counter plot of P.D.E.% mass of catalyst vs concentration of dye

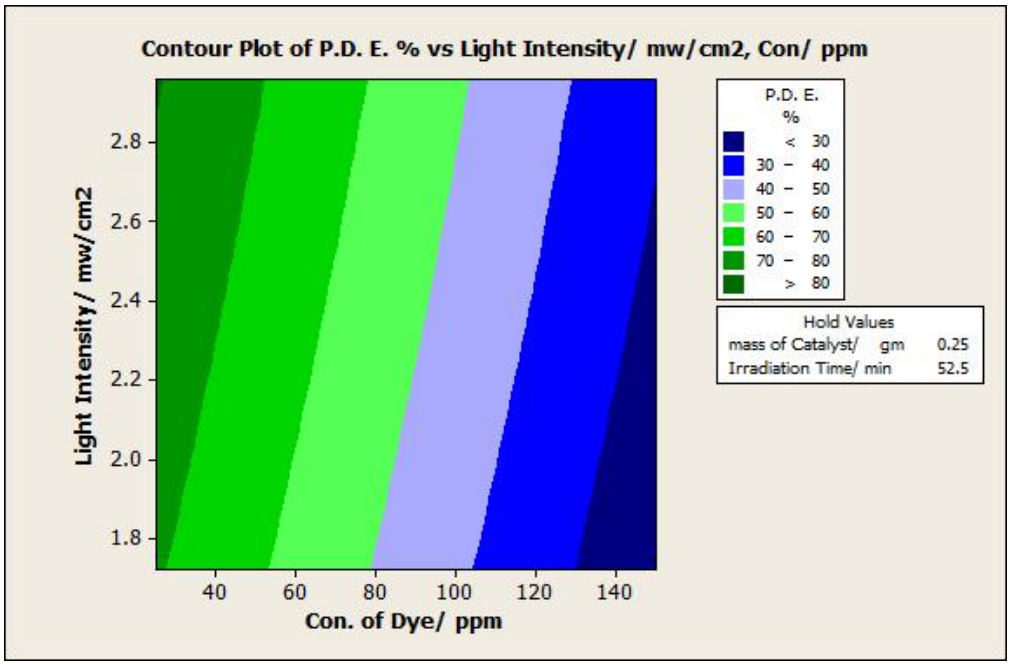

Figure(3-24) Counter Plot P.D.E. % Ligh Intensity vs Concentration of Dye

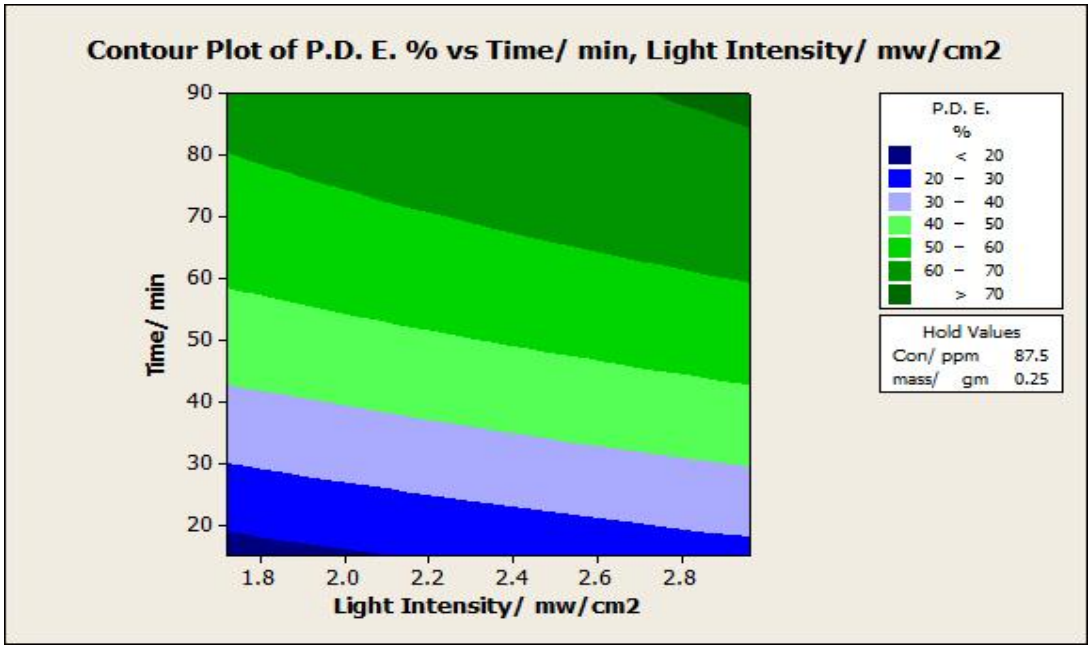

Figure(3-25):Counter plot P.D.E. % irradiation time vs light intensity

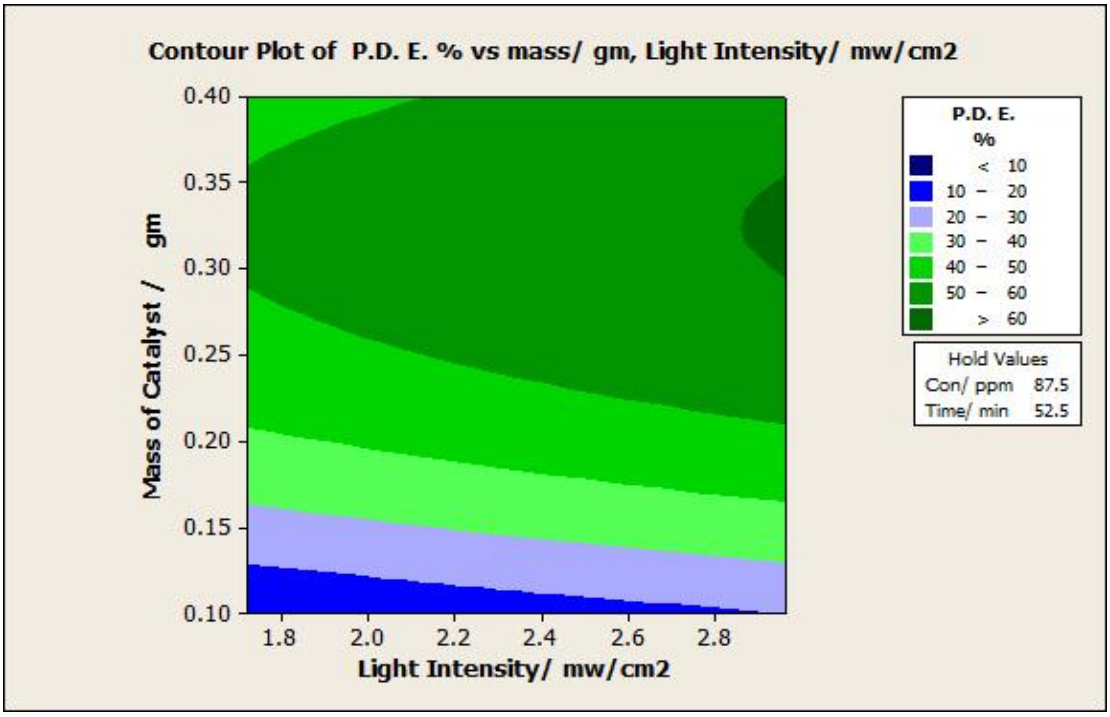

Figure(3-26): Counter plot P.D.E.% mass of catalyst vs light intensity

In our results show the RSM model is a helpful technique for the optimum conditions design. Also, it was in a good agreement with the predicted result, which confirms the adequacy and validity of the model. Results of RSM optimization for the photo degradation efficiency of MG are showed in Table (3-1). As seen from the RSM results, the highest degradation performance of MG occurs at optimal conditions mention in each figure.

3.4 Conclusions

1. The prepared TiO_2 show good photocatalytic activity for removal of dyes
2. Silver doped of TiO_2 shows the highest photo catalysis in our study
3. When light intensity increased the photo degradation increase.
4. When pollutants concentration increased the photo degradation decreased
5. When initial dye concentration increase the photo catalytic degradation gradually decrease.
6. It can be considered H_2O_2 as a good scavenger for pollutant
7. Clear shift shows by using DR/spectrophotometer after Ag doping on the surface of TiO_2
8. Can be reuse photocatalytic Ag/TiO_2 with good efficiency, this activity reduced with time
9. Response surface methodology which through can used to find the highest removal of dyes through optimization of parameters such as amount of catalyst, light intensity, concentration of dyes, and reaction time

3.5 Suggestions for Further Study

1. Using other metals doping on semiconductors, such as M (Pt, Au, Cu; Pd, Fe) on TiO_2 Surface, for enhanced optical and photocatalytic properties.
2. Using a new a type of lights as a sources of photo-degradations (UVA and visible light on the Ag/TiO_2 surface)
3. Using the prepared surface for the degradation of drug and phenolic compounds
4. Using the prepared surface as a model for antibacterial activity

References

Reference

1. Leung, D.Y., *Outdoor-indoor air pollution in urban environment: challenges and opportunity.* Frontiers in Environmental Science, 2015. **2**: p. 69.
2. Chaudhry, F.N. and M. Malik, *Factors affecting water pollution: a review.* J Ecosyst Ecography, 2017. **7**(22 :(5p. 1-3.
3. Rafiq, A., et al., *Photocatalytic degradation of dyes using semiconductor photocatalysts to clean industrial water pollution.* Journal of Industrial and Engineering Chemistry, 2021. **97**: p. 111-128.
6. Banerjee, S. and M. Chattopadhyaya, *Adsorption characteristics for the removal of a toxic dye, tartrazine from aqueous solutions by a low cost agricultural by-product.* Arabian Journal of Chemistry, 2017. **10**: p. S1629-S1638.
5. Khanna, A. and V. Shetty K, *Solar light-driven photocatalytic degradation of Anthraquinone dye-contaminated water by engineered Ag@ TiO2 core–shell nanoparticles.* Desalination and Water Treatment, 2015. **54**(3): p. 744-757.
6. Van Aken, P., et al., *Advances in ozonation and biodegradation processes to enhance chlorophenol abatement in multisubstrate wastewaters: a review.* Environmental Science: Water Research & Technology, 2019. **5**(3): p. 444-481.
7. Bashir, A., et al., *Removal of heavy metal ions from aqueous system by ion-exchange and biosorption methods.* Environmental Chemistry Letters, 2019. **17**(2): p. 729-754.
8. Hube, S., et al., *Direct membrane filtration for wastewater treatment and resource recovery: A review.* Science of the total environment, 2020. **710**: p. 136375.
9. Wang, H., et al., *Effective adsorption of dyes on an activated carbon prepared from carboxymethyl cellulose: Experiments, characterization and advanced modelling.* Chemical Engineering Journal, 2021. **417**: p. 128116.
10. Shubha, J.P., et al., *Facile green synthesis of semiconductive ZnO nanoparticles for photocatalytic degradation of dyes from the textile industry: A kinetic approach.* Journal of King Saud University-Science, 2022. **34**(5): p. 102047.
11. Manou, L., et al., *What does "Nanoscience–Nanotechnology" mean to primary school teachers?* International Journal of Science and Mathematics Education, 2022. **20**(6): p. 1269-1290.

12. Reza, K.M., A. Kurny, and F. Gulshan, *Parameters affecting the photocatalytic degradation of dyes using TiO2: a review.* Applied Water Science, 2017. **7**(4): p. 1569-1578.
13. Kolahalam, L.A., et al., *Review on nanomaterials: Synthesis and applications.* Materials Today: Proceedings, 2019. **18**: p. 2182-2190.
14. Rohilla, D., S. Chaudhary, and A. Umar, *An overview of advanced nanomaterials for sensor applications.* Engineered Science :16 .2021 ،p. 47-70.
15. Saleh, T.A., *Nanomaterials: Classification, properties, and environmental toxicities.* Environmental Technology & Innovation, 2020. **20**: p. 101067.
16. Singh, V., P. Yadav, and V. Mishra, *Recent advances on classification, properties ،synthesis, and characterization of nanomaterials.* Green synthesis of nanomaterials for bioenergy applications, 2020: p. 83-97.
17. Darweesh, H.H.M., *Nanomaterials: Classification and Properties-Part I.* Journal of Nanoscience, 2018. **1**(1): p. 1-11.
18. Jamkhande, P.G., et al., *Metal nanoparticles synthesis: An overview on methods of preparation, advantages and disadvantages, and applications.* Journal of drug delivery science and technology, 2019. **53**: p. 101174.
19. Ashley, A., et al., *Emerging investigator series: photocatalytic membrane reactors: fundamentals and advances in preparation and application in wastewater treatment.* Environmental Science: Water Research & Technology, 2022. **8**(1): p. 22-46.
20. Al Mayyahi, A. and H.A.A. Al-Asadi, *Advanced oxidation processes (AOPs) for wastewater treatment and reuse: a brief review.* Asian J. Appl. Sci. Technol, 2018. **2**: p. 18-30.
21. Poyatos, J.M., et al., *Advanced oxidation processes for wastewater treatment: state of the art.* Water, Air, and Soil Pollution, 20 :205 .10p. 187-204.
22. Byrne, J.A., et al., *A review of heterogeneous photocatalysis for water and surface disinfection.* Molecules, 2015. **20**(4): p. 5574-5615.
23. Hayder, I., et al., *Degradation and inactivation of ciprofloxacin by photocatalysis using TiO2 nanoparticles.* J. App. Pharm, 2012. **4**: p. 487-497.
24. Jaafar, N., et al., *Direct in situ activation of Ag0 nanoparticles in synthesis of Ag/TiO2 and its photoactivity.* Applied Surface Science, 2015. **338**: p. 75-84.
25. Mishra, A., A. Mehta, and S. Basu, *Clay supported TiO2 nanoparticles for photocatalytic degradation of environmental pollutants: A review.* Journal of environmental chemical engineering, 2018. **6**(5): p. 6088-6107.

26. Aljeboree, A.M., et al., *Adsorption of textile dyes in the presence either clay or activated carbon as a technological models: A review.* Journal of Critical Reviews, 2020. **7**(5): p. 620-626.
27. A. Demirbas, *Agricultural based activated carbons for the removal of dyes from aqueous solutions: a review* J. Hazard. Mater., 2009 :167 .p. 1-9.
28. Jasim, L.S., N.D. Radhy, and H.O. Jamel, *Synthesis and characterization of poly (acryl amide - Maleic acid) hydrogel: Adsorption kinetics of a malachite green from aqueous solutions.* Eurasian Journal of Analytical Chemistry, 2018. **13**(1.(
29. S. Nethaji a, b., A. Sivasamya,, G. Thennarasua, S. Saravananb, *Adsorption of Malachite Green dye onto activated carbon derived from Borassus aethiopum flower biomass.* Journal of Hazardous Materials, 2010. **181** p. 271–280.
30. Oguzie, E., et al., *Corrosion inhibition and adsorption behavior of malachite green dye on aluminum corrosion.* Chemical Engineering Communications, 2010. **198**(1): p. 46-60.
31. Fox, M.A. and M.T. Dulay, *Heterogeneous photocatalysis.* Chemical reviews, 1993. **93**(1): p. 341-357.
32. Dima, R.S., et al., *Electronic, structural, and optical properties of mono-doped and Co-Doped (210) TiO2 brookite surfaces for application in dye-sensitized solar cells—a first principles study.* Materials, 2021. **14**(14): p. 3918.
33. Allen, N.S., et al., *The effect of crystalline phase (anatase, brookite and rutile) and size on the photocatalytic activity of calcined polymorphic titanium dioxide (TiO2).* Polymer degradation and stability, 2018. **150**: p. 31-36.
34. Sanjines, R., et al., *Electronic structure of anatase TiO2 oxide.* Journal of Applied Physics, 1994. **75**(6): p. 2945-2951.
35. Safety, C.P., *Health Effects Due to Titanium Nanoparticles in Food and Toothpaste Cannot be Excluded.* 2016.
36. Haynes, W.M., D.R. Lide, and T.J. Bruno, *CRC handbook of chemistry and physics*. 2016: CRC press.
37. Hitosugi, T., et al., *Properties of TiO2- based transparent conducting oxides.* Physica status solidi (a), 2010. **207**(7): p. 1529-1537.
38. Challagulla, S., et al., *TiO2 synthesized by various routes and its role on environmental remediation and alternate energy production.* Nano-Structures & Nano-Objects, 2017. **12**: p. 147-156.
.39 Wang, S., et al., *Titanium-defected undoped anatase TiO2 with p-type conductivity, room-temperature ferromagnetism, and remarkable*

photocatalytic performance. Journal of the American Chemical Society, 2015. **137**(8): p. 2975-2983.
40. Peiris, S., et al., *Recent development and future prospects of TiO2 photocatalysis.* Journal of the Chinese Chemical Society, 2021. **68**(5): p. 738-769.
41. Gao, M ،.et al., *Anatase TiO2 nanocrystals via dihydroxy bis (ammonium lactato) titanium (IV) acidic hydrolysis and its performance in dye-sensitized solar cells.* Journal of Porous Materials, 2018. **25**(5): p. 1499-1504.
42. Suchanek, W.L. and R.E. Riman. *Hydrothermal synthesis of advanced ceramic powders*. in *Advances in Science and Technology*. 2006. Trans Tech Publ.
43. Yang, G. and S.-J. Park, *Conventional and microwave hydrothermal synthesis and application of functional materials: A review.* Materials, 2019. **12**(7 :(p. 1177.
44. Yang, S. and L. Gao, *Fabrication and characterization of nanostructurally flowerlike aggregates of TiO2 via a surfactant-free solution route: effect of various reaction media.* Chemistry letters, 2005. **34**(7): p. 1044-1045.
45. Lu, X., Z. Yue, and B. Peng, *Preparation of TiO2-nanotube-based photocatalysts and degradation kinetics of patulin in simulated juice.* Journal of Food Engineering, 2022. **323**: p. 110992.
46. Mamaghani, A.H., F. Haghighat, and C.-S. Lee, *Hydrothermal/solvothermal synthesis and treatment of TiO2 for photocatalytic degradation of air pollutants: Preparation, characterization, properties, and performance.* Chemosphere, 2019. **219**: p. 804-825.
47. Sundar, K.P. and S. Kanmani, *Progression of Photocatalytic reactors and it's comparison: A Review.* Chemical Engineering Research and Design, 2020. **154**: p. 135-150.
48. Pino, E., et al., *Photocatalytic degradation of aqueous rhodamine 6G using supported TiO2 catalysts. A model for the removal of organic contaminants from aqueous samples.* Frontiers in chemistry, 2020. **8**: p. 365.
49. Szczepanik, B., *Photocatalytic degradation of organic contaminants over clay-TiO2 nanocomposites: A review.* Applied Clay Science, 2017. **141**: p. 227-239.
50. Jin, Y., et al., *High photocatalytic activity of spent coffee grounds derived activated carbon-supported Ag/TiO2 catalyst for degradation of organic dyes and antibiotics.* Colloids and Surfaces A: Physicochemical and Engineering Aspects, 2022. **655**: p. 130316.
.51 Sabir, A., T.A. Sherazi, and Q. Xu, *Porous polymer supported Ag-TiO2 as green photocatalyst for degradation of methyl orange.* Surfaces and Interfaces, 2021. **26**: p. 101318.

52. Wahyuni, E.T., R. Roto, and M. PrameSwari, *TiO2/Ag-nanoparticle as a Photocatalyst for Dyes Degradation*. 2017.
53. Wang ،T., et al., *Preparation of electrospun Ag/TiO2 nanotubes with enhanced photocatalytic activity based on water/oil phase separation.* Physica E: Low-dimensional Systems and Nanostructures, 2017. **86**: p. 103-110.
54. Hirano, M., et al., *Direct Formation of Zirconia- Doped Titania with Stable Anatase- Type Structure by Thermal Hydrolysis.* Journal of the American Ceramic Society, 2002. **85**(5): p. 1333-1335.
55. Falaras, P., et al., *Enhanced activity of silver modified thin-film TiO2 photocatalysts.* International Journal of Photoenergy, 2003. **5**(3): p. 123-130.
56. Orlov, A., et al., *Photocatalytic properties of TiO2 modified with gold nanoparticles in the degradation of 4-chlorophenol in aqueous solution.* Catalysis letters, 2004. **92**(1): p. 41-47.
57. Barakat, M ،.G. Hayes, and S.I. Shah, *Effect of cobalt doping on the phase transformation of TiO2 nanoparticles.* Journal of nanoscience and nanotechnology, 2005. **5**(5): p. 759-765.
58. Jang, J.S., et al., *A composite photocatalyst of CdS nanoparticles deposited on TiO* 2*nanosheets.* Journal of nanoscience and nanotechnology, 2006. **6**(11): p. 3642-3646.
59. Rengaraj, S., et al. *Heterogeneous photocatalytic degradation of chlorophenols over Ag-TiO2 nano particles in an aqueous suspension*. in *Solid State Phenomena*. 2007. Trans Tech Publ.
60. Wang, W., et al., *Preparation and photocatalytic properties of Fe3+-doped Ag@ TiO2 core–shell nanoparticles.* Journal of Colloid and Interface Science, 2008. **323**(1): p. 182-186.
61. Chuang, H.-Y. and D.-H. Chen, *Fabrication and photocatalytic activities in visible and UV light regions of Ag@ TiO2 and NiAg@ TiO2 nanoparticles.* Nanotechnology, 2009. **20**(10): p. 105704.
62. Xiang, Q., et al., *Microwave- hydrothermal preparation and visible- light photoactivity of plasmonic photocatalyst Ag- TiO* 2*nanocomposite hollow spheres.* Chemistry–An Asian Journal, 2010. **5**(6): p. 1466-1474.
63. Ashkarran, A.A., S.M. Aghigh, and N.J. Farahani, *Visible light photo-and bioactivity of Ag/TiO2 nanocomposite with various silver contents.* Current Applied Physics :(4)11 .2011 ،p. 1048-1055.
64. Wang, D., et al., *Preparation of TiO 2 loaded with crystalline nano Ag by a one-step low-temperature hydrothermal method.* Journal of Materials Chemistry, 2012. **22**(32): p. 16306-16311.

65. Alkaim, A.F., et al., *Solvent-free hydrothermal synthesis of anatase TiO2 nanoparticles with enhanced photocatalytic hydrogen production activity.* Applied Catalysis A: General, 2013. **466**: p. 32-37.
66. Yang, Y., et al., *Photocatalytic activity of Ag–TiO2-graphene ternary nanocomposites and application in hydrogen evolution by water splitting.* International Journal of Hydrogen Energy, 2014. **39**(15): p. 7664-7671.
.67 Lian, Z., et al., *Plasmonic silver quantum dots coupled with hierarchical TiO2 nanotube arrays photoelectrodes for efficient visible-light photoelectrocatalytic hydrogen evolution.* Scientific reports, 2015. **5**(1): p. 1-10.
.68 Gao, L., et al., *A robust superhydrophobic antibacterial Ag–TiO2 composite film immobilized on wood substrate for photodegradation of phenol under visible-light illumination.* Ceramics International, 2016. **42**(2): p. 2170-2179.
.69 Saeed, K., et al., *Efficient photodegradation of methyl violet dye using TiO2/Pt and TiO2/Pd photocatalysts.* Applied Water Science, 2017. **7**(7): p. 3841-3848.
70. Mozafari, H. and S .Azarakhsh, *Photodegradation of azo dyes: photocatalyst and magnetic investigation of CoFe2O4–TiO2–Ag nanocomposites.* Journal of Materials Science: Materials in Electronics, 2018. **29**(7): p. 5993-6003.
71. Hong, D., et al., *Plasmonic Ag@ TiO2 core–shell nanoparticles for enhanced CO2 photoconversion to CH4.* ACS Sustainable Chemistry & Engineering, 2019. **7**(23): p. 18955-18964.
72. Güy, N., et al., *Boosting visible light response and charge separation by plasmonic Ag and TiO2 modification of Ag3VO4 for degradation of pollutants.* Water Science and Technology, 2020. **82**(9): p. 1912-1920.
73. Zhang, G., et al., *Facile synthesize hierarchical tubular micro-nano structured AgCl/Ag/TiO2 hybrid with favorable visible light photocatalytic performance.* Journal of Alloys and Compounds, 2021. **855**: p. 157512.
74. Razavi, F.S., D. Ghanbari, and M. Salavati-Niasari, *Comparative Study on the Role of Noble Metal Nanoparticles (Pt and Pd) on the Photocatalytic Performance of the BaFe12O19/TiO2 Magnetic Nanocomposite: Green Synthesis, Characterization, and Removal of Organic Dyes under Visible Light.* Industrial & Engineering Chemistry Research, 2022. **61**(36): p. 13314-13327.
75. Cherif, Y., et al., *Facile Synthesis of Gram-Scale Mesoporous Ag/TiO2 Photocatalysts for Pharmaceutical Water Pollutant Removal and Green Hydrogen Generation.* ACS omega, 2023.
76. Khan, H., et al., *Experimental methods in chemical engineering: X‐ ray diffraction spectroscopy—XRD.* The Canadian Journal of Chemical Engineering, 2020. **98**(6): p. 1255-1266.

77. Havrdova, M., et al., *Field emission scanning electron microscopy (FE-SEM) as an approach for nanoparticle detection inside cells.* Micron, 2014. **67**: p. 149-154.
78. Spurgeon, S.R., et al., *Towards data-driven next-generation transmission electron microscopy.* Nature materials, 2021. **20**(3): p. 274-279.
79. Yazidi A Atrous, M.E.S., Felycia S Lotfi , Smadji E Suryadi , Alessandro B Petriciolet , Luiz D Guilherme , Ben L Abdelmottaleb, *Adsorption of amoxicillin and tetracycline on activated carbon prepared from durian shell in single and binary systems: Experimental study and modeling analysis.* Chemical Engineering Journal, 2020. **379**: p. 122320.
80. Dutta, A., *Fourier transform infrared spectroscopy.* Spectroscopic methods for nanomaterials characterization, 2017: p. 73-93.
81. Rocha, F.S., et al., *Experimental methods in chemical engineering: Ultraviolet visible spectroscopy—UV- Vis.* The Canadian Journal of Chemical Engineering, 2018. **96**(12): p. 2512-2517.
82. Abraham, J., et al., *Thermoanalytical techniques of nanomaterials*, in *Characterization of nanomaterials*. 2018, Elsevier. p. 213-236.
83. Makuła, P., M. Pacia, and W. Macyk, *How to correctly determine the band gap energy of modified semiconductor photocatalysts based on UV–Vis spectra*. 2018, ACS Publications. p. 6814-6817.
84. Souza, I.P., et al., *Optimization of thermal conditions of sol-gel method for synthesis of TiO2 using RSM and its influence on photodegradation of tartrazine yellow dye.* Journal of Environmental Chemical Engineering, 2021. **9**(2 :(p. 104753.
85. Zhang, Y., et al., *One-step synthesis of Ag@ TiO2 nanoparticles for enhanced photocatalytic performance.* Nanomaterials, 2018. **8**(12): p. 1032.
86. Zhang, J., et al., *Aerosol processing of Ag/TiO2 composite nanoparticles for enhanced photocatalytic water treatment under UV and visible light irradiation.* Ceramics International, 2022. **48**(7): p. 9434-9441.
87. Tsega, M. and F. Dejene, *Morphological, thermal and optical properties of TiO2 nanoparticles: The effect of titania precursor.* Materials Research Express, 2019. **6**(6): p. 065041.
88. Van Viet, P., et al., *The fabrication of the antibacterial paste based on TiO2 nanotubes and Ag nanoparticles-loaded TiO2 nanotubes powders.* Journal of Experimental Nanoscience, 2017. **12**(1): p. 220-231.
89. Nyamukamba, P., et al., *Silver/carbon codoped titanium dioxide photocatalyst for improved dye degradation under visible light.* International Journal of Photoenergy, 2017. **2017**.

90. Boxi, S.S. and S. Paria, *Visible light induced enhanced photocatalytic degradation of organic pollutants in aqueous media using Ag doped hollow TiO 2 nanospheres.* RSC Advances, 2015. **5**(47): p. 37657-37668.
91. Pathak, G., et al., *Analysis of photoluminescence, UV absorbance, optical band gap and threshold voltage of TiO2 nanoparticles dispersed in high birefringence nematic liquid crystal towards its application in display and photovoltaic devices.* Journal of Luminescence, 2017. **192**: p. 33-39.
92. Nainani, R., P. Thakur, and M. Chaskar, *Synthesis of silver doped TiO2 nanoparticles for the improved photocatalytic degradation of methyl orange.* J. Mater. Sci. Eng. B, 2012. **2**(1): p. 52-58.
93. Yang, S., et al., *A facile fabrication of hierarchical Ag nanoparticles-decorated N-TiO2 with enhanced photocatalytic hydrogen production under solar light.* international journal of hydrogen energy, 2016. **41**(5): p. 3446-3455.
94. Sambaza, S., A. Maity, and K. Pillay, *Enhanced degradation of BPA in water by PANI supported Ag/TiO2 nanocomposite under UV and visible light.* Journal of Environmental Chemical Engineering, 2019. **7**(1): p. 102880.
95. Nguyen, T.H., et al., *Green synthesis of a photocatalyst Ag/TiO2 nanocomposite using Cleistocalyx operculatus leaf extract for degradation of organic dyes.* Chemosphere, 2022. **306**: p. 135474.
96. Aljobree ،A.M., A.F. et al. , *ZnONanoparticles as a model for removal of Phrmaceutical compounds(Vitamin B12)in the presence of UV light.* International Journal of Recent Technology and Engineering(IJRTE), 2019. **8**(2S3.(
97. Abdelaal, M. and R. Mohamed, *Novel Pd/TiO2 nanocomposite prepared by modified sol–gel method for photocatalytic degradation of methylene blue dye under visible light irradiation.* Journal of Alloys and Compounds, 2013. **576**: p. 201-207.
98. Shan, R., et al., *Photocatalytic degradation of methyl orange by Ag/TiO2/biochar composite catalysts in aqueous solutions.* Materials Science in Semiconductor Processing, 2020. **114**: p. 105088.
99. Saeed, M., et al., *Azadirachta indica leaves extract assisted green synthesis of Ag-TiO2 for degradation of Methylene blue and Rhodamine B dyes in aqueous medium.* Green Processing and Synthesis, 2019. **8**(1): p. 659-666.
100. Alkaim, A.F.a.F.H.H., *Photocatalytic degradation of EDTAby using TiO2 suspension.* International Journal of Chemical Science, 2012. **10(1)**: p. 586-5.98

101. Kulkarni, R.M., et al., *Ag-TiO2 nanoparticles for photocatalytic degradation of lomefloxacin.* Desalination and Water Treatment, 2016. **57**(34): p. 16111-16118.
102. Zhang, M., et al., *Recyclable Ag/TiO2@ PDMS Coated Cotton Fabric with Visible-Light Photocatalytic for Efficient Water Purification.* 2021.
103. Nosaka, Y. and A.Y. Nosaka, *Generation and detection of reactive oxygen species in photocatalysis.* Chemical reviews, 2017. **117**(17): p. 11302-11336.

الخلاصة

تتكون هذه الرسالة من ثلاثة أجزاء ،اولا تم تصنيع جزيئات TiO_2 النانوية باستخدام الطريقة الحرارية المائية ، وتحميل سطح TiO_2بمعدن نبيل الفضة عن طريق الترسيب الضوئي. هنا تم تحضير الجسيمات النانوية من نوع الاناتاز عبر طريقة حرارية مائية أحادية الخطوة باستخدام المحاليل المائية من التيتانيوم (IV) مكرر (أمونيوم لاكتاتو) ثنائي هيدروكسيد المتوفرة تجاريا مع محلول الامونيا بتركيز(3 مولاري) تم تشخيص الخصائص الكيميائية والفيزيائية للمركبات النانوية المحضرة باستخدام تقنيات مختلفة مثل انحراف الأشعة السينية (XRD) ,المجهر الالكتروني النافذ (TEM) ,المجهر الالكتروني الماسح (SEM) والتحليل الطيفي للانعكاس الانعكاسي للأشعة فوق البنفسجية المرئية.

كانت نتائج SEM,TEM تشير الى وجود تكتلات عالية لل TiO2 ونسبة قليلة منAg على سطح TiO2 ،لذلك لم تظهر نتائجXRD أي قمم لـ Ag أظهرت تقنية الأشعة فوق البنفسجية –المرئية أن فجوة الطاقة لأكسيد التيتانيوم اختزلت واصبحت اقل بعد اضافة الفضة.

الجزء الثاني حيث يتناول التحطم التحفيزي الضوئي لمحلول مائي من صبغة المليخايت الاخضر التي تمت دراستها في ظل ظروف مختلفة في وجود جزيئات Ag / TiO_2 النانوية. هناك تأثير لعوامل المختلفة مثل تأثير تركيز صبغة المليخايت الاخضر ، تأثير وزن المركب النانوي Ag / TiO_2 ، شدة الضوء ، دور أنواع الأكسجين الفعالة ، تأثير التجديد التجريبي وإزالة نموذج المختبر (خليط من عدة أصباغ) من محلول مائي.

أوضحت النتائج ان كفاءة التحطم التحفيزي الضوئي تزداد بزيادة كمية المحفز من 1،.غم الى 4،. غم وايضا اظهرت ارتفاع معدل التحطم التحفيزي الضوئي مع انخفاض تركيز صبغة المليخايت الاخضر. والزيادة في شدة الضوء تؤدي إلى زيادة معدل التحطم التحفيزي الضوئي أيضًا دور H_2O_2(بيروكسيد الهيدروجين) ككاسح ومحطم لصبغة المليخايت الاخضر ، المحفز الضوئي Ag / TiO_2 له خاصية التنظيف الذاتي والقدرة على إعادة الاستخدام مما يجعلها واعدة للمعالجة البيئية

الجزء الأخير من هذه الرسالة يتعلق بمنهجية سطح الاستجابة ، حيث وجد ايضا تأثير استخدام تراكيز مختلفة من صبغة الملكيت الخضراء مع استخدام شدة ضوء مختلفة باستخدام كمية من المحفز(Ag/TiO_2). حيث أظهرت النتائج عند التطبيق النظري أن كفاءة التحطم الضوئي يتناسب تناسبا عكسيًا مع تركيز الصبغة المستخدم . وزيادة شدة الضوء تؤدي إلى زيادة التحطم الضوئي من هنا تمت المقارنة بين النتائج النظرية والنتائج العملية

وزارة التعليم العالي والبحث العلمي

جامعة بابل / كلية العلوم للبنات

قسم الكيمياء

تحضيرمواد النانوية من Ag/TiO_2 للتحطيم الضوئي التحفيزي لصبغة المليخايت الاخضر،التحسين من خلال منهجية سطح الاستجابة

رسالة مقدمة إلى

مجلس كليــة العلوم للبنات في جامعــة بابــل وهي جـزء من
متطلبات نيل درجــة الماجستير في الكيمياء

تقدمت بها

زينب صالح مهدي ناجي

بكالوريوس في الكيمياء
جامعة بابل (2001-2002م)

بإشراف

أ.د اياد فاضل القيم

1444هـ **2023م**